ABSTRACT

Jiong Lin. Assessing the Value of Model Calibration for Signalized Intersections. (Under the direction of Dr. Nagui Rouphail.)

The Highway Capacity Manual (HCM) provides the most widely used methodologies for evaluating the quality of service on highway and street facilities. However, many users contend that the HCM models they are using are not accurate in emulating some real world conditions. In this thesis, the HCM control delay model for signalized intersections is assessed to identify where and when such deficiencies occur.

Four signalized intersections within the Chicago central business district (CBD) area are selected to assess the accuracy of the HCM control delay model. The lane groups studied include three through lane groups and one permissive left-turn lane group. Input data (e.g. lane group volumes, proportion of vehicles arriving on green, effective green time, etc.) for the HCM model and empirical data (e.g. actual measured control delay) were collected cycle by cycle in the field. Saturation flow rates estimated from (a) the HCM default parameter values, (b) field calibration and (c) statistical optimization are entered into the HCM control delay model, respectively, to calculate control delays. Then, the control delays calculated from the model are contrasted to those measured from the field.

For the through lane groups, the analysis indicates that the control delay calculated using the HCM default parameter values overestimates field delay in most of cases, and it may not accurately reflect the lane groups' performance. However, when field calibrated and/or optimized values are used, the control delay estimated using the model is close to that obtained

from field measurements, and this indicates that the HCM control delay model is reliable. For the permissive left-turn lane group, no matter which values of saturation flow rate are used, the control delay estimated using the HCM model is not comparable with that obtained from field measurements due to the small sample size of the number of vehicles arriving per cycle, and other factors apparently not reflected in the delay model.

ASSESSING THE VALUE OF MODEL CALIBRATION FOR SIGNALIZED INTERSECTIONS

by

JIONG LIN

A thesis submitted to the Graduate Faculty of
North Carolina State University
In partial fulfillment of the requirements for
The Degree of Master of Science

CIVIL, CONSTRUCTION, AND ENVIRONMENTAL ENGINEERING

Raleigh, NC

2004

APPROVED BY:

Dr. Joseph E. Hummer	Dr. Billy M. Williams

Dr. Nagui M. Rouphail
Chair of Advisory Committee

BIOGRAPHY

Jiong Lin was born in Beijing, China. After graduation from Northern Jiaotong University in Beijing, China, where she received a Bachelor of Science degree in Transportation Engineering in July 1995, she worked for Civil Aviation Management Institute of China as an assistant professor for eight years. In September 2001, she received her Master of Business Administration (Aviation Management) degree from Royal Melbourne Institute of Technology, Melbourne, Australia. In August 2003, she enrolled at North Carolina State University to pursue a Master of Science degree in Civil Engineering with a transportation engineering concentration.

ACKNOWLEDGEMENTS

Many people have assisted me in the completion of my graduate thesis. I would first like to acknowledge Dr. Nagui Rouphail, my academic advisor, who had spent a lot of time and spirits with me on the thesis structure formulation, provided guidance on research materials. His constructive and most helpful comments on my thesis draft deserve to be sincerely appreciated.

I would also like to thank Dr. Joseph Hummer and Dr. Billy Williams for serving on my thesis committee and giving suggestions for ways to improve my research.

Last, I would like to thank my husband, Xuejun, for his understanding and support. Without his encouragement and proofreading, this thesis would not have been possible.

TABLE OF CONTENTS

List of Tables

List of Figures

CHAPTER 1. INTRODUCTION

1.1 Background

The Highway Capacity Manual (HCM) published by the Transportation Research Board provides traffic engineers and researchers alike with the most widely used methodologies for evaluating the quality of service on highway and street facilities. It is the primary document presenting methods for assessing capacity and level of service for elements of the surface transportation system not only in the United States, but also in many other countries in the world. The first edition of the HCM was published in 1950. The second and third editions were published in 1965 and 1985, respectively. The latest edition of the HCM was published in 2000.

A continuing concern about the HCM procedures is the following: are the models presented in the HCM reliable enough and applicable to all highway and street facilities under a variety of operating conditions? A sound model should reflect real world conditions. Many users contend that the HCM models they are using are not accurate, and the models have some limitations in emulating some real world conditions. While one cannot expect the models to fit all empirical data, there is a need for a rigorous assessment of where and when such deficiencies occur.

1.2 Problem Statement

By far, the most widely used chapter in the HCM is the signalized intersection analysis. In particular the control delay model for signalized intersections is the key to estimate the level of service (LOS) at all signalized intersections. A host of variables and parameters need to be input to the model in order to calculate control delay. Some of the variables can be measured directly from the field, such as intersection geometry, intersection signal timing, and lane group volumes, etc. For those that cannot be directly measured from the field, HCM default values or derivative

values are typically used. Lane group saturation flow rate, one of the most important variables, is a typical derivative variable that enters into the calculation of control delay. That variable is derived from the functional relationship between an ideal saturation flow rate and several adjustment factors including lane widths, heavy vehicle percentages, number of bus stops, pedestrian volumes, number of parking maneuvers, etc.

The HCM recommends the use of a locally calibrated saturation flow rate wherever possible. The implication is that a properly calibrated model will yield an acceptable delay estimate and consequently a more realistic level of service. This assumption needs to be verified against field observations. Since the delay model parameters including the saturation flow rate can be directly observed in the field (e.g. demand, duration of the analysis period), it can be assumed that any discrepancies between the observed and estimated HCM delay may be due to errors in the delay model formulation itself.

1.3 Objectives and Scope

The nature of traffic operations at signalized intersections may vary from site to site, such as traffic flow, drivers' characteristics, and intersection geometry, etc. The purpose of this research is to assess the HCM 2000 control delay model for signalized intersections with various un-calibrated and calibrated saturation flow rates. Input data (e.g. lane group volumes, proportion of vehicles arriving on green, effective green time, cycle length, etc.) for the HCM model and empirical data (e.g. actual measured control delay) are collected from the field. Saturation flow rates estimated from (a) HCM formulae, (b) field calibration and (c) statistical optimization are entered into HCM 2000 control delay model, respectively, to calculate control delays. Then, the

control delays calculated from the model are compared to the control delay measured from the field. The following questions are to be answered at the end of this research:

- To what extent does the un-calibrated HCM saturation flow rate and corresponding delay estimate adequately predict field delay at signalized intersections?
- What is gained, in terms of prediction power, by using a field calibrated saturation flow rate and delay model parameters?
- What is the remaining error in predicting control delay when an optimal saturation flow rate and delay parameters are used? and,
- Are there differences in delay estimation for through and permitted left-turn lane groups?

Four signalized intersections within Chicago central business district (CBD) area are selected for this research. All signals selected are pre-timed. The lane groups being studied include three through lane groups and a permissive left-turn lane group. Traffic data were collected cycle by cycle during one-hour study period. Instead of peak 15-minute analysis period, the length of one cycle is used as the unit of analysis period to estimate average control delay in the HCM control delay model. Comparison and analysis of saturation flow rates, distribution of control delay, and distribution of level of service (LOS) are conducted to evaluate the reliability and applicability of the HCM 2000 control delay model.

1.4 Organization

There are five chapters in this thesis. Chapter 1 is the introduction. Literature review is provided in Chapter 2, which includes the HCM methodology and other methods of model calibration and validation. Chapter 3 introduces the methodology that is employed in this research and a description of data collection for the intersections. Chapter 4 discusses the results for the studied

lane groups, in which the assessment of the reliability of the HCM 2000 control delay model is performed. In the final part, Chapter 5, uncertainties of the HCM 2000 control delay model are analyzed and conclusions of this research are drawn.

CHAPTER 2. LITERATURE REVIEW

The HCM 2000 control delay model for signalized intersections is reviewed in this chapter. Three methodologies for model calibration and validation are also reviewed. Koutsopoulos et al. (2) summarize the general statistical methods to validate traffic models. Rouphail et al. (3, 4) use microscopic simulation to assess a generalized delay model that is based on HCM 1994 delay model. Sacks et al. (5, 6) apply a Bayesian methodology to calibrate and validate the HCM 2000 control delay model. The estimation of permissive left-turn capacity is much more complicated, which is effected by the opposing flow. Mousa et al. (7) discuss the effect of opposing platoon on permissive left-turn capacity.

2.1 HCM Methodology

The HCM 2000 (1) defines control delay at signalized intersections as the average control delay experienced by all vehicles that arrive in the analysis period, including delays incurred beyond the analysis period when the lane group is oversaturated. The HCM 2000 control delay model for signalized intersections includes three parts: uniform delay, incremental delay, and initial queue delay. HCM 2000 (1) describes the average control delay per vehicle for a given lane group as:

$$d = d_1(PF) + d_2 + d_3 \qquad \text{Eq. (2.1)}$$

where

d = control delay per vehicle (sec/veh);

d_1 = uniform control delay assuming uniform arrivals (sec/veh);

PF = uniform delay progression adjustment factor, which accounts for effects of signal progression;

d_2 = incremental delay to account for effect of random arrivals and oversaturation queues, adjusted for duration of analysis period and type of signal control; this delay component assumes that there is no initial queue for lane group at start of analysis period (sec/veh); and

d_3 = initial queue delay, which accounts for delay to all vehicles in analysis period due to initial queue at start of analysis period (sec/veh).

The progression adjustment factor is determined by the proportion of vehicles arriving on green. Good progression means that most vehicles arrive on green and the average delay per vehicle is low. On the other hand, with poor progression, most vehicles arrive on red and experience longer delay at the intersection. The progression adjustment factor in HCM 2000 (1) is defined as:

$$PF = \frac{(1-P)f_{PA}}{1-(g/C)} \qquad \text{Eq. (2.2)}$$

where

P = proportion of vehicles arriving on green;

g = effective green time (sec);

C = cycle length (sec); and

f_{PA} = supplemental adjustment factor for early and late platoons arriving during green.

The proportion of vehicles arriving on green may be either measured in the field or estimated from arrival type.

2.1.1 Uniform Delay

The estimate of uniform delay in HCM 2000 (1) is based on the assumptions of uniform arrivals (stable flow) and no initial queue. It is based on the first term of Webster's delay model (8).

$$d_1 = \frac{0.5C(1-g/C)^2}{1-[\min(1,X)g/C]} \quad \text{Eq. (2.3)}$$

where X is the volume/capacity ratio or degree of saturation for lane group, which is given by:

$$X = v/c = vC/sg \quad \text{Eq. (2.4)}$$

where

v = demand flow rate for lane group (veh/h);

s = saturation flow rate for lane group (veh/h); and

c = capacity of lane group (veh/h).

X values beyond 1.0 are not applicable in the computation of uniform delay, but are transferred to the second delay term, d_2.

2.1.2 Incremental Delay

As presented in HCM 2000 (1), the incremental delay accounts for non-uniform arrivals, temporary cycle failures, and oversaturated flow conditions. HCM 2000 (1) defines incremental delay as

$$d_2 = 900T\left[(X-1)+\sqrt{(X-1)^2+\frac{8kIX}{cT}}\right] \quad \text{Eq. (2.5)}$$

where

d_2 = incremental delay to account for effect of random and oversaturation queues, adjusted for duration of analysis period and type of signal control (sec/veh); this delay component assumes that there is no initial queue for lane group at the start of analysis period;

T = duration of analysis period (h);

c = lane group capacity (veh/h);

k = incremental delay factor that is dependent on controller settings and v/c ratio; and

I = upstream filtering/metering adjustment factor.

According to the definition given by HCM 2000 (1), the parameter k is included in the above equation to incorporate the effect of controller type on delay. For pre-timed signals, a value of k = 0.5 is used, which is based on a queuing process (M/D/1) with random arrivals and uniform service time equivalent to the lane group capacity. The incremental delay adjustment factor accounts for the effects of filtered arrivals from upstream signals. The default value of I =1 is based on the assumption that arrivals each cycle follow a Poisson distribution so that the variance in arrivals equals the mean. An I-value of less than 1.0 is used for nonisolated intersections. This reflects how an upstream signal could decrease the variance in the number of arrivals per cycle at the subject intersection. Incremental delay is sensitive to the degree of saturation for lane group (X). When X>1.0, the control delay increases dramatically.

2.1.3 Initial Queue Delay

When there is unmet demand at the end of an analysis period, where the volume/capacity ratio is greater than 1.0, an initial queue occurs at the beginning of the following analysis period. Vehicles arriving in this following time period inevitably experience additional delay since the initial queue must first clear the intersection. In these cases, the initial queue delay must be considered. HCM 2000 (1) estimates initial queue delay using the following equation,

$$d_3 = \frac{1800 Q_b (1+u\ )t}{cT} \qquad \text{Eq. (2.6)}$$

where

Q_b = the initial queue at the start of period T (veh);

c = lane group capacity (veh/h);

T = duration of analysis period (h);

t = duration of unmet demand in T (h); and

u = delay parameter.

The parameters t and u are estimated by the following equations:

$$t = 0 \text{ if } Q_b = 0, \text{ else } t = \min\left\{T, \frac{Q_b}{c[1-\min(1,X)]}\right\}, \text{ and}$$

$$u = 0 \text{ if } t<T, \text{ else } u = 1 - \frac{cT}{Q_b[1-\min(1,X)]}$$

When there is initial queue, the computation of uniform control delay (d_1) must be evaluated using X = 1.0 for the period (t) during which the initial queue clear the intersection and using the actual X value for the remainder of the analysis period (T-t). In these cases, a time-weighted value of d_1 is used, as indicated below,

$$d_1 = d_s * \frac{t}{T} + d_u * PF * \frac{(T-t)}{T} \qquad \text{Eq. (2.7)}$$

where

d_s = saturated delay (i.e. d_1 evaluated for X = 1.0); and

d_u = undersaturated delay (i.e. d_1 evaluated for actual X value).

2.2 General Statistical Validation Methods

Statistical methods are widely used in the process of model calibration and validation. Comparisons between field observations and results from model calculations using statistical methods give analysts significant confidence on whether the model is effective or not. Koutsopoulos et al. (2) suggest that the selection of appropriate methods and their application for validating traffic models depends on the nature of the output data. Single-valued measures of performance (MOPs), for example, average delay, are appropriate for small-scale application in which one statistic summarizes the performance of a traffic network system. Multivariate MOPs, for example, time-dependent flow, capture the temporal and/or spatial distribution of a MOP to describe the dynamics of a system. Three statistical approaches for model validation are discussed.

- Goodness-of-fit measures

  Statistics including root mean square error (RMSE), root mean square percent error (RMSPE), mean error (ME), and mean percent error (MPE) can be used as goodness-of-fit measures to evaluate the overall performance of traffic models.

  RMSE and RMSPE penalize large errors at a higher rate relative to small errors. These two measures are given by:

$$RMSE = \sqrt{\frac{1}{N}\sum_{n=1}^{N}(Y_n^{\text{mod}} - Y_n^{obs})^2} \qquad \text{Eq. (2.8)}$$

$$RMSPE = \sqrt{\frac{1}{N}\sum_{n=1}^{N}\left(\frac{Y_n^{\text{mod}} - Y_n^{obs}}{Y_n^{obs}}\right)^2} \qquad \text{Eq (2.9)}$$

  where Y_n^{obs} and Y_n^{mod} are the averages of observed and model estimated measurements at space-time point n, respectively calculated from all available data.

ME and MPE indicate the existence of systematic under-prediction or over-prediction in the model estimated measurements. They are given by:

$$ME = \frac{1}{N}\sum_{n=1}^{N}(Y_n^{\mathrm{mod}} - Y_n^{obs}) \qquad \text{Eq. (2.10)}$$

$$MPE = \frac{1}{N}\sum_{n=1}^{N}\frac{(Y_n^{\mathrm{mod}} - Y_n^{obs})}{Y_n^{obs}} \qquad \text{Eq. (2.11)}$$

ME and MPE are more useful when applied to measurements at each point in space than to all measurements jointly.

Koutsopoulos et al. (2) state another measure, Theil's inequality coefficient, U, which provides information on the relative error. It is given by:

$$U = \frac{\sqrt{\frac{1}{N}\sum_{n=1}^{N}(Y_n^{\mathrm{mod}} - Y_n^{obs})^2}}{\sqrt{\frac{1}{N}\sum_{n=1}^{N}(Y_n^{\mathrm{mod}})^2} + \sqrt{\frac{1}{N}\sum_{n=1}^{N}(Y_n^{obs})^2}} \qquad \text{Eq. (2.12)}$$

where U is bounded ($0 \le U \le 1$). $U = 0$ implies a perfect fit between the observed and modeled measurements. $U = 1$ implies the worst possible fit.

- Hypothesis testing and Confidence intervals

  Besides the classic hypothesis tests, such as two-sample t-test, Mann-Whitney test, and two-sample Kolmogorov-Smirnov test, Koutsopoulos et al. (2) recommend using test for the equality of the mean of observed and modeled measurements, by which no assumptions like normal distribution and/or equal variance are needed. The statement of hypothesis is given as following:

  $H_0: \overline{Y}^{\mathrm{mod}} = \overline{Y}^{obs}$ against $H_1: \overline{Y}^{\mathrm{mod}} \neq \overline{Y}^{obs}$ at the α significance level, reject H_0 if:

$$\frac{\left|\overline{Y}^{\,\mathrm{mod}} - \overline{Y}^{\,obs}\right|}{\sqrt{\frac{(s^{\mathrm{mod}})^2}{n^{\mathrm{mod}}} + \frac{(s^{obs})^2}{n^{obs}}}} \geq t_{\alpha/2,\hat{f}} \qquad \text{Eq. (2.13)}$$

where $\overline{Y}^{\,obs}, \overline{Y}^{\,\mathrm{mod}}, s^{obs}$, and s^{mod} are the sample means and standard deviations of the observed and model estimated measurements, respectively. n^{obs} and n^{mod} are the corresponding sample size. $\hat{f}$ is the modified number of degrees of freedom, and is given by:

$$\hat{f} = \frac{\left(\frac{s^{\mathrm{mod}}}{n^{\mathrm{mod}}} + \frac{s^{obs}}{n^{obs}}\right)^2}{\frac{(s^{\mathrm{mod}})^4}{(n^{\mathrm{mod}})^2(n^{\mathrm{mod}}-1)} + \frac{(s^{obs})^4}{(n^{obs})^2(n^{obs}-1)}} \qquad \text{Eq. (2.14)}$$

The corresponding (1-α) confidence interval is given by:

$$(\overline{Y}^{\,\mathrm{mod}} - \overline{Y}^{\,obs}) \pm t_{\alpha/2,\hat{f}} \sqrt{\frac{(s^{\mathrm{mod}})^2}{n^{\mathrm{mod}}} + \frac{(s^{obs})^2}{n^{obs}}} \qquad \text{Eq. (2.15)}$$

Koutsopoulos et al. (3) also discuss a regression procedure that can be used to validate traffic models using an F-test of the joint equality of the means and variances of the field and modeled measurements. Assuming there are *N* different input data sets, for pairs of observations $(y_n^{obs}, y_n^{\mathrm{mod}})$, *n = 1, …, N,* the following regression is performed:

$$(y_n^{obs} - y_n^{\mathrm{mod}}) = \beta_0 + \beta_1 (y_n^{obs} + y_n^{\mathrm{mod}}) + \varepsilon_n \qquad \text{Eq. (2.16)}$$

The hypothesis that the observed and model outputs are drawn from identical distributions is tested with the null H_0: $\beta_0 = 0$ and $\beta_1 = 0$.

2.3 Validation Using Microscopic Simulation Model

Usually, a comparison between field observed data and model calculated results is one of the most effective methods to assess traffic models. In some cases, however, it is extremely difficult to obtain field data due to various limitations, for instance, limited availability of funds. For these cases, other methods may be used, from which the outputs are considered the same as or very close to data obtained through field observation. Rouphail et al. (3, 4) propose a generalized delay model for inclusion in the update of HCM 1994, where the TRAF-NETSIM microscopic simulation model is used to verify this delay model for oversaturated conditions and for vehicle-actuated traffic signals.

In this case, TRAF-NETSIM outputs were compared with field data for undersaturated conditions and were found to be in general agreement. A total of 180 scenarios were analyzed in Rouphail et al.'s research (3), and 20 replications were conducted for each scenario with different random-number seeds to obtain a reasonably accurate estimate of the average delay. Delay curves for analysis periods of 15- and 30-min for HCM 1994 delay model, generalized delay model, and TRAF-NETSIM simulation model were plotted together in a figure. The plot indicates that the generalized delay model corresponds closely to the simulated delay values, but the HCM model doesn't. A conclusion is drawn that the proposed generalized delay model is more suitable than the HCM 1994 delay equation for use under oversturated conditions.

For validating the generalized delay model for vehicle-actuated traffic signals (4), similar inputs (such as traffic volumes, average queue discharge headway, and average signal timings) were entered into TRAF-NETSIM and the generalized delay model. Delay values obtained from TRAF-NETSIM were compared with those estimated by the model. Regression analysis was

performed and plots of TRAF-NETSIM delays against model estimated delays for all volume levels and signalization alternatives were generated. The analysis and plots show that the mean square error (mean of the squared difference between simulated delay and model delay) is low and the slope of the regression line passing through the origin is close to 1.0. This indicates that the generalized model delays and TRAF-NETSIM delays are comparable.

In addition, the delays calculated from the HCM 1994 delay model and the generalized model were compared with delay data collected from the field (4). Regression analysis indicates that the mean square error for the HCM 1994 delay model is almost twice of that for the generalized delay model. The slope of the regression line passing through the origin for the generalized model delays is closer to 1.0 than that for the HCM 1994 model delays. It is evident from the mean square errors and slopes that the delay values estimated with the generalized model are closer to values observed in the field than the delays estimated by the HCM 1994 delay model.

Since the generalized delay model and TRAF-NETSIM yield comparable delays and the generalized model delays were comparable to field observed delays, a conclusion is drawn that the generalized delay model is an improvement over the HCM 1994 delay model for estimating delays at vehicle-actuated traffic signals.

2.4 Bayesian Analysis

Bayarri et al (5) point out that a model is a biased representation of reality and accounting for this bias is the central issue for model validation. Furthermore, models alone could not provide evidence of bias. Either expert opinion or field data is necessary to assess the bias – they focus on the latter. Let x_i be the input and u be the tuning parameters. They statistically model "reality = model + bias" as:

$$y^R(x_i) = y^M(x_i, u) + b(x_i) \quad \text{Eq. (2.17)}$$

When field data $x_1, x_2, \ldots, x_n$ are obtained, the model is:

$$y^F(x_i) = y^R(x_i) + \varepsilon_i^F = y^M(x_i, u) + b(x_i) + \varepsilon_i^F \quad \text{Eq. (2.18)}$$

where: y^F and y^M denote field and model outputs, respectively, $y^R(x_i)$ the value of "real" process at input x_i, $b(x_i)$ the model bias which is an unknown function and treating it requires non-standard techniques, and ε_i^R the independent normal random errors with mean zero and variance λ^F.

Batista Paulo et al. (6) used the Bayesian methodology in calibrating and validating the HCM control delay model. The parameters that can be obtained by calibration through the use of field data are classified into three categories: a) parameters that can be directly estimated, perhaps with error, from field data; b) parameters not directly measurable; and c) tuning parameters that are not "real" but are required by the model. According to this research (6), Bayesian analysis provides an attractive path to simultaneously calibrate the parameters of type (a), (b) and (c) and deal with the possible presence of model bias. Therefore, calibration and assessment of validity can be done in one combined analysis. Bayesian analysis determines the posterior distribution of model parameters and inputs, given the observed field data. The resulting distribution will then reflect the actual uncertainty in the parameters and inputs, adjudicate between the tuning parameters and the possible model bias thereby providing resistance to over-tuning, and quantify and assess the model bias.

To predict the real process, $y^R(x_i)$, Batista Paulo et al. (6) used the bias-corrected prediction to verify the delay model. At given x,

$$\hat{y}^R(x) = \frac{1}{N}\sum_{n=1}^{N}\left[y^M(x, u_i) + b_i(x)\right] \quad \text{Eq. (2.19)}$$

Assuming u was the posterior mean of the tuning parameters, they defined the pure model prediction of reality with the estimate of the bias, $\hat{b}(x)$, as

$$\hat{b}(x) = \hat{y}^R(x) - y^M(x,\hat{u}) \qquad \text{Eq. (2.10)}$$

Tolerable difference was also introduced to indicate if the model was reliable for the reality. The expression is stated as (6):

$$\Pr\left[\left|"reality" - prediction\right| \le \delta\right] > \alpha \qquad \text{Eq. (2.21)}$$

where δ is the tolerable difference, and α is the acceptable probability. For the bias-corrected prediction, the expression can be stated as (15):

$$\Pr\left[\left|y^M(x,u_i) + b_i(x) - \hat{y}^R(x)\right| \le \delta\right] > \alpha \qquad \text{Eq. (2.22)}$$

If δ is small enough within the probability α, the model is valid. If δ is greater than a tolerable value, the model may not be reliable.

2.5 Effect of Opposing Flow on permissive Left-turn Capacity

The estimation of permissive left-turn capacity is much more complicated than that for through movements, which not only depends on the conditions of the approach but also on the opposing flow. Mousa et al. (7) indicates that the observed left-turn capacity is inversely proportional to the platoon ratio and flow rate on the opposing approach, e.g. progression for through traffic may have an adverse effect on the opposing permissive left-turns.

Left-turn data were measured in an exclusive left-turn lane which was opposed by one lane of through traffic. Data were collected only from cycles when left-turn queues spilled over to the next cycle (i.e. demand > capacity). They examined data through several regression models to determine whether there was an effect of measured parameters on the permissive left-turn capacity. The regression results showed that the estimate of the permissive left-turn capacity decreased as opposing flow rate increased and good progression on the opposing approach resulted in a decrease in left-turn capacity during the green phase.

In addition, Mousa et al. (7) performed two analyses to validate the 1985 HCM left-turn capacity estimation procedure with field data, the 1985 HCM procedure with default saturation flow rates and the 1985 HCM procedure with saturation flow rates estimated from field observations. It was found that the ratio of observed to 1985 HCM capacities decreased as progression of opposing flow improved. This indicates that the 1985 HCM method may overestimate left-turn capacities under these conditions relative to the poor progressive situations.

2.6 Summary of Literature Review

The 2000 HCM control delay model for signalized intersection, which includes three terms, uniform delay, incremental delay, and initial queue delay, is described in this chapter. Methods for model calibration and validation are also reviewed. Koutsopoulos et al. (2) summarized a few widely used statistical methods in the process of model calibration and validation, including goodness-of-fit measures, hypothesis testing and confidence interval. Rouphail et al. (3,4) used microscopic simulation model (TRAF-NETSIM) to validate a generalized delay model and the 1994 HCM control delay model for oversaturated conditions and for vehicle-actuated traffic signals, because it was considered that the simulation model could reflect the field situations. Batista Paulo et al. (6) applied the Bayesian methodology to calibrate and validate the HCM 2000 control delay model. Since the Bayesian methodology can simultaneously calibrate the particular parameters and deal with the possible presence of model bias, the calibration and validation can be done in one combined analysis. The data used in Rouphail et al.'s and Batista Paulo et al.'s research for the HCM control delay model calibration and validation were collected from through lane group only. The permissive left-turn situation was not considered. Mousa et al.'s (7) research focused on the analysis of permissive left-turn capacity. It indicates that the

improvement of progression on the opposing approach can cause a decrease of left-turn capacity. Most of the studies reviewed are focused on the methodologies and procedures of the HCM delay model calibration and validation. However, there is no published research on assessing the value of the HCM control delay model calibration for signalized intersections.

CHAPTER 3. METHODOLOGY AND DATA

This chapter describes the methodology employed in this research to assess the HCM control delay model. Various un-calibrated and calibrated saturation flow rates are used in the HCM delay model to calculate model delays, and the model delays are then compared with field measurements. Data collection for four selected lane groups is described, including intersection configuration, traffic volume, signal display, and so on.

3.1 Method Description

In the HCM control delay model for signalized intersections, the input parameters, including cycle length (C), effective green time (g), analysis period (T), traffic flow rate (v), proportion of vehicles arriving on green (P), and initial queue (Q_b), are measured directly from the field. Cycle length (75seconds) is used as the duration of analysis period (T) instead of the 15-minute period that is used in most other studies using the HCM methodology, since the measurement of average field delay in this research is based on cycle by cycle measurements.

The degree of saturation (X) is determined by lane group saturation flow rate (s) because g and C are fixed for pre-timed signals. The HCM procedure uses the default ideal saturation flow rate with considerations of adjustments for other factors to compute the lane group saturation flow rate. It may or may not reflect the field situation. The alternatives use field calibrated and statistically optimized saturation flow rates.

In the incremental delay (d_2) equation, the incremental delay factor (k) and upstream filtering/metering adjustment factor (I) are difficult to directly measure in the field. Because k and I appear together in this equation, they are treated as one parameter in this research.

Then, the HCM control delay model can be described as (see Section 2.1 for definitions of the parameters):

$$PF(P) = \frac{(1-P)f_{PA}}{1-(g/C)} \quad \text{Eq. (3.1)}$$

$$d_1(v,s) = \frac{0.5C(1-g/C)^2}{1-[\min(1,X)g/C]} = \frac{0.5C(1-g/C)^2}{1-\left[\min\left(1,.vC/sg\right)g/C\right]} \quad \text{Eq. (3.2)}$$

$$d_2(v,s,kI) = 900T\left[(X-1)+\sqrt{(X-1)^2+\frac{8kIX}{cT}}\right] \quad \text{Eq. (3.3)}$$

$$d_3(v,Q_b,s) = \frac{1800Q_b(1+u\ )t}{cT} \quad \text{Eq. (3.4)}$$

where v, P, Q_b are input variables for the model, and they change from cycle to cycle. s and kI are the two tuning parameters in the HCM delay model and they are assumed to be constant for individual intersections during the one-hour study period. The total control delay in the i^{th} cycle with no initial queue presence ($Q_b = 0$) is given by

$$d^{Model}(v_i,P_i,s,kI) = d_1(v_i,s)PF(P_i) + d_2(v_i,s,kI) \quad \text{Eq. (3.5)}$$

The total control delay in the i^{th} cycle where an initial queue is present ($Q_b>0$) is given by

$$d^{Model}(v_i,P_i,Q_{b,i},s,kI) = 0.5C(1-g/C)\frac{t_i}{T} + d_1(v_i,s)PF(P_i)\frac{T-t_i}{T} + d_2(v_i,s,kI) + d_3(v_i,Q_{b,i},s)$$

Eq. (3.6)

As the output, delays estimated by the HCM model (d^{Model}) are to be compared to delays measured from the field (d^{Field}). If the difference between model delay and the mean field measured delay ($\overline{d}^{Field}$) is within the specified tolerable range, a conclusion can be drawn that

the HCM delay model reflects the real world situation. On the other hand, if the comparison shows significant differences between the model delay and the mean field measured delay, e.g. the difference is out of the specified tolerable range, the HCM control delay model may not be comparable to the field measurement for the particular lane group. The following expression can be used for assessing the reliability of the model,

$$\Pr\left(\left|d^{Model} - \bar{d}^{Field}\right| \le \delta\right) > \alpha \qquad \text{Eq. (3.7)}$$

where δ is the maximum difference, and α is assurance level (acceptable probability).

The "traditional" statistic, mean square error (MSE), is selected to assess the goodness-of-fit of control delay on a cycle-by-cycle basis.

$$MSE = \frac{1}{N}\sum_{i=1}^{N}\left[y^{Field}(v_i, P_i, Q_{bi}) - y^{Model}(v_i, P_i, Q_{bi}, s, kI)\right]^2 \qquad \text{Eq. (3.8)}$$

where N is the number of cycles observed. The smaller the value of MSE, the smaller the difference between the delays obtained from the HCM model and field measurement.

The HCM control delay model parameters, s and kI, are specified first before assessing the HCM control delay model, and they are estimated using three different methods in this research.

- Estimate s and kI using HCM 2000 Equation with Default Values

  The default value of ideal saturation flow rate, s, is 1900veh/h/ln in HCM 2000(1). Given the effects of other factors, such as proportion of heave vehicles, lane utilization, etc., the adjusted saturation flow rate is described in HCM 2000 (1) as

  $$s = s_{ideal} \cdot N \cdot f_w \cdot f_{HV} \cdot f_g \cdot f_p \cdot f_{bb} \cdot f_a \cdot f_{LU} \cdot f_{LT} \cdot f_{RT} \cdot f_{Lpb} \cdot f_{Rpb} \qquad \text{Eq. (3.9)}$$

  s = adjusted saturation flow rate for subject lane group (veh/h);

  s_{ideal} = base saturation flow rate per lane (pc/h/ln). Default value is 1900veh/h/ln;

  N = number of lanes in lane group;

f_w = adjustment factor for lane width;

f_{HV} = adjustment factor for heavy vehicles in traffic stream;

f_g = adjustment factor for approach grade;

f_p = adjustment factor for existence of a parking lane and parking activity adjacent to lane group;

f_{bb} = adjustment factor for blocking effect of local buses that stop within intersection area;

f_a = adjustment factor for area type;

f_{LU} = adjustment factor for lane utilization;

f_{LT} = adjustment factor for left turns in lane group;

f_{RT} = adjustment factor for right turns in lane group;

f_{Lpb} = pedestrian adjustment factor for left-turn movements; and

f_{Rpb} = pedestrian-bicycle adjustment factor for right-turn movements.

As specified in HCM 2000 (1), the default k value 0.5 is used in HCM delay model for pre-timed signals. The default value of I is equal to 1 with the assumption of a Poisson arrival process. So $kI = 0.5$ is used in the HCM model to calculate control delay.

- Calibrate s and kI from Field Observations

Saturation flow rate is the maximum queue discharge rate, which can be obtained from discharge headways measured in the field. Discharge headways of queuing vehicles are measured cycle by cycle in the field. For lane groups in which more than one lane are included, discharge headways for the lane with the highest saturation flow rate are used. The method of measuring saturation flow rates is described in Section 3.3. Field

calibrated saturation flow rate refers to the average of measured saturation flow rates for all cycles.

For intersections with a pre-timed signal, $k = 0.5$ is used. The parameter I is affected by filtered arrivals from upstream signals. Usually, an I-value less than 1.0 is used for nonisolated intersections. The I-value can be calculated from field data as the ratio of the variance to the mean number of arrivals per cycle for the subject lane group. The number of vehicles arriving vary across cycles and intersections. Different I-values are used for the lane groups studied in this research.

- Optimize s and kI

A range of saturation flow rate is specified for each lane group and the range for an individual lane group may be different from that for others. For intersections with a pre-timed signal $k = 0.5$ is used. And usually, an I-value less than 1.0 is used for nonisolated intersections. Therefore, the range of the kI value can be specified as 0.1 through 0.5 in increments of 0.1. The control delay MSEs are calculated using Equation 3.8 with different combinations of saturation flow rate s and kI. The saturation flow rate that minimizes MSE is the optimized saturation flow rate for a particular value of kI. In other words, the delay calculated using the optimized saturation flow rate for a particular value of kI is the closest value to the control delay measured in the field.

3.2 Data Collection and Description

Four signalized intersections located in the Chicago central business district (CBD) area are selected for the study. One of the characteristics of a CBD area is that traffic flow is very high

during peak hours. The delays during peak hours are longer than that during any other time period of a day and are reasonably easy to measure. Information of vehicles passing through the intersections was recorded by video cameras set on the roof of nearby buildings during the AM or PM peak hour on May 25th, 2000 and September 27th, 2000. Traffic data including volumes, effective green time, and saturation flow rate, etc. for lane groups studied in this research were manually extracted from the video.

Data collected from the field (video) for each intersection/movement studied include:

- Cycle Length: For all intersections studied, the cycle length is 75 seconds. That is, there were 48 cycles in AM or PM peak hour during which data were collected.
- Effective Green Time: Effective green time for each studied movement was measured cycle by cycle. The duration of effective green time is from the time when the front axle of the first vehicle crosses the stop bar after the beginning of green time to the time when the front axle of the last vehicle crosses the stop bar before the end of yellow time, and the following vehicle has to stop to wait for the next green time. Since driver behavior varies, e.g. some are aggressive but some are conservative, the effective green time for the same movement may vary from cycle to cycle. The difference may be even more than a few seconds. The average effective green time for each movement in each cycle is used to calculate control delays using the HCM model.
- Intersection Timing Plan: Intersection timing plan includes green time, yellow time, and all red time, all of which varied from intersection to intersection.
- Lane Width: Information cannot be obtained from the field. Twelve-foot lane width was assumed for all intersections.
- Number of Lanes: Number of lanes was different for the studied intersections.

- Number of Vehicles Arriving per Cycle: Measured.
- Number of Heavy Vehicles and Buses: Measured.
- Number of Vehicles Arriving on Green per Cycle: For each cycle, the number of vehicles that arrive at stop line or join the queue (stationary or moving) while the green signal is displayed was counted.
- Bus Stops: No bus stopping at the intersections was observed during the data collection periods.
- Parking Maneuvers: No parking within 250 feet of the intersection was permitted in the lane groups studied.
- Queuing Vehicle Discharging Headway: Headways were measured to obtain saturation flow rate for the studied movements. See Section 3.3 for a detailed description of field measurement of saturation flow rate.
- Number of Vehicles Delayed per Cycle. See Section 3.4 for the detailed description of field measurement of control delay at signalized intersections.

Traffic information was collected cycle by cycle. Thus 48 sets of data for each studied lane group were collected for analysis.

3.2.1 Wells-Grand Intersection

Wells St. is a one-way north-south street where traffic flows from north to south. Grand Ave. is an east-west street with two-way traffic. Figure 3.1 shows the intersection configuration and the signal timing plan. The southbound through lane group on Wells St. was selected for analysis. There are two approaching lanes and two receiving lanes for southbound through movement.

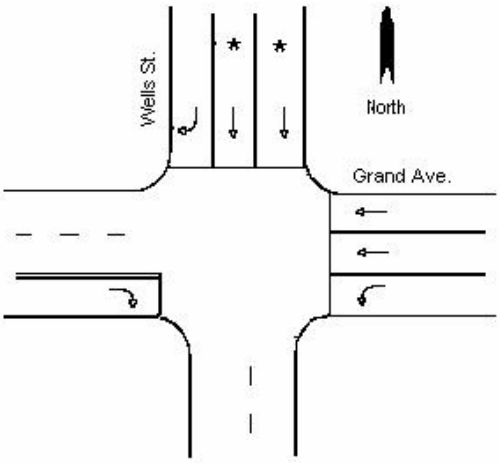

a) Intersection Configuration *(* subject lane group)*

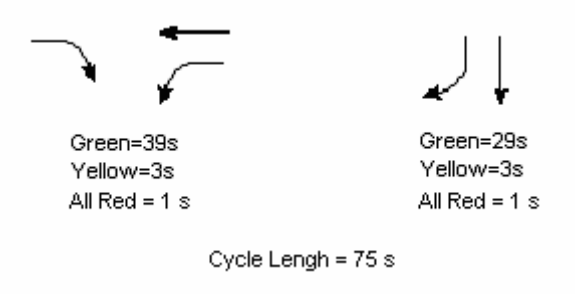

b) Signal Timing Plan

Figure 3.1 Wells-Grand Intersection Configurations and Signal Timing Plan

Traffic data for the AM peak hour (7:50am-8:50am) on May 25th, 2000 were collected cycle by cycle. See Table A.1 in Appendix A for a summary of field data. The southbound through movement had poor progression during the AM peak hour. In most cycles, more than 50 percent of vehicles arrived on red. Vehicles experienced longer delay compared to movements that had good progression. No oversaturated conditions occurred during the AM peak hour. In other words, there was no initial queue which occurred at the beginning of the green phase in any cycle.

Therefore, when the control delays are calculated using the HCM control delay model, the initial queue delay component did not need to be considered.

There were cycles in which uncommon factors affected vehicles that discharged during the green time. They are labeled “unusual cycles”. The delay in these cycles may be longer than that in “other cycles”. The “unusual cycles” include:

- Cycle 5, 15, 17, 23, and 27: In these cycles, a downstream queue blocked vehicles from discharging at the intersection. The southbound vehicles could not pass through the intersection or had to move slowly at the beginning of the green phase of these cycles, thus significantly reducing the saturation flow rate.
- Cycle 6: An emergency vehicle entered the intersection from the north during the green time. Vehicles in both through lanes stopped aside to let it proceed.
- Cycle 42: A construction vehicle traveling from east to west blocked the intersection while the southbound movement had a green phase. Southbound vehicles on both through lanes had to stop until the intersection was cleared.

3.2.2 LaSalle-Ohio Intersection

LaSalle St. is a north-south street with two-way traffic. Ohio St. is an east-west street with one-way traffic from west to east. Figure 3.2 shows the intersection configuration and signal timing plan. The southbound through movement on LaSalle St. was selected for analysis. There are three approaching lanes and three receiving lanes for the southbound though movement.

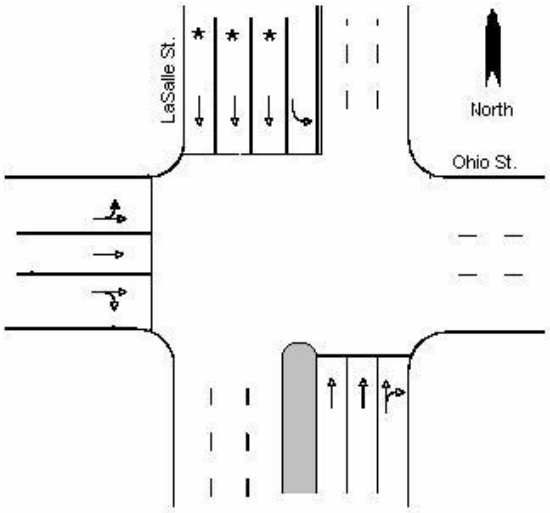

a) Intersection Configuration *(* subject lane group)*

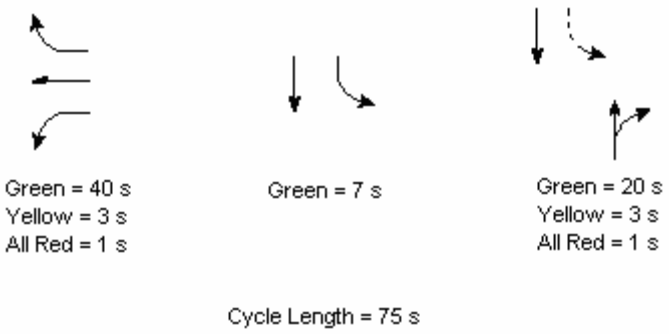

b) Signal Timing Plan

Figure 3.2 LaSalle-Ohio Intersection Configurations and Signal Timing Plan

Traffic data for the AM peak hour (7:30am-8:30am) on Sep. 27th, 2000 were collected cycle by cycle. See Table A.2 in Appendix A for the summary of field data. The southbound through movement had good progression for most of cycles during the Am peak hour, e.g. more than 50 percent of the vehicles arrived on green. Oversaturation occurred in some cycles during the AM peak hour due to heavy through traffic. In other words, an initial queue was present at the beginning of red phase in some cycles. When control delay is calculated using the HCM delay model, the initial queue delay component needs to be added for these cycles.

Only one unusual cycle appeared during the AM peak hour. In Cycle 12, a police car entered the intersection from the north during green time and all southbound vehicles stopped for a few seconds to let it pass through.

3.2.3 LaSalle-Ontario Intersection

LaSalle St. has been described in the previous section. Ontario St. is one block to the north of Ohio St., which is an east-west road with one-way traffic from east to west. Figure 3.3 shows the intersection configuration and signal timing plan. The northbound through movement on LaSalle St. was selected for analysis. There are three approaching lanes and three receiving lanes for the southbound though movement.

Traffic data for the PM peak hour (5:05pm-6:05pm) on Sep. 27th, 2000 were collected cycle by cycle. See Table A.3 in Appendix A for the summary of field data. Because northbound through traffic was heavy and the distance between this intersection and the downstream intersection was quite short, downstream queues didn't clear in time and caused the northbound through traffic not to discharge efficiently during the green time in some cycles. As a result, capacity decreased in these cycles and an initial queue occurred in the following cycles. For the cycles in which an initial queue was present, the initial queue delay component must be considered when control delay is calculated using the HCM delay model. In addition, since there were parked vehicles and a bus stop on the northbound rightmost receiving lane, most vehicles used the left two through lanes in order to avoid being blocked. The poor lane utilization made the left two through lanes more congested. Sixteen cycles in

which vehicles experienced longer delay due to downstream queue include Cycles 16, 23, 29 through 36, 38, 40, 42, 44, 46, and 47.

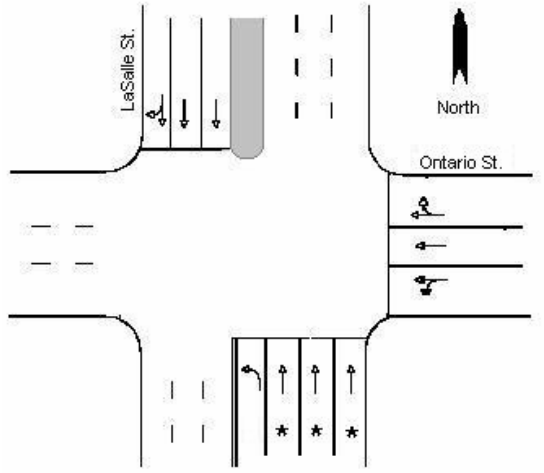

a) Intersection Configuration *(* subject lane group)*

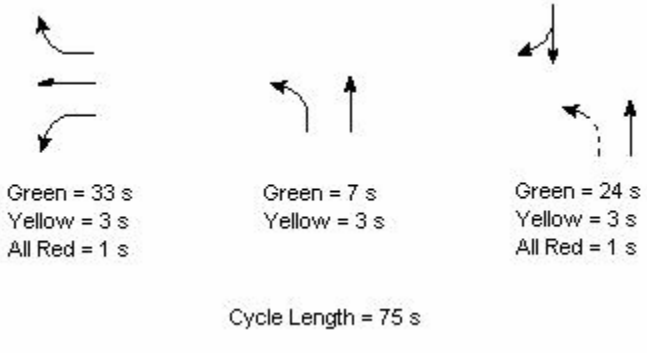

b) Signal Timing Plan

Figure 3.3 LaSalle-Ontario Intersection Configurations and Signal Timing Plan

3.2.4 LaSalle-Grand Intersection

LaSalle St. has been described in Section 3.2.2. Grand Ave. is a block to the south of Ohio St., which is an east-west road with one-way traffic from east to west. Figure 3.4 shows the intersection configuration and signal timing plan. The northbound left-turn movement on

LaSalle St. was selected for analysis. There is one exclusive northbound left-turn lane on LaSalle St. and the signal phase for this movement is permissive only.

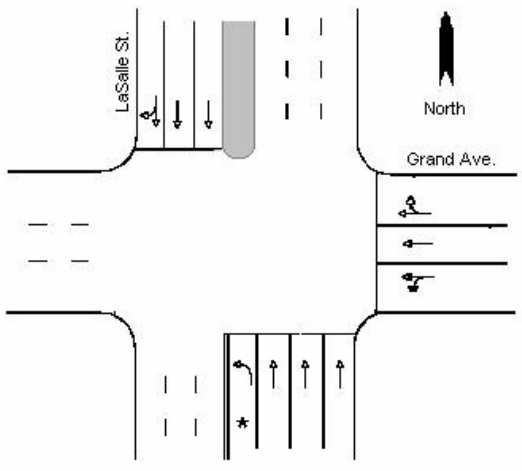

a) Intersection Configuration *(* subject lane group)*

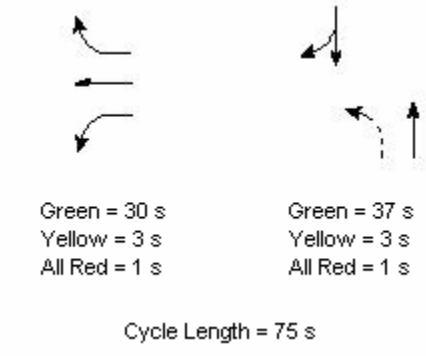

b) Signal Timing Plan

Figure 3.4 LaSalle-Grand Intersection Configurations and Signal Timing Plan

Traffic data for AM peak hour (from 8:50AM to 9:50AM) on Sep. 27th, 2000 were collected cycle by cycle. Since there were no left-turn vehicles arriving in Cycle 20, 26 and 31, data for 45 cycles were analyzed. See Table A.4 in Appendix A for the summary of field data. Because the signal phase for northbound left-turn traffic is permissive only, left-turn vehicles have to wait

until opposing queuing vehicles discharge and acceptable gaps in that stream appear. Since opposing traffic had excellent progression, left-turn vehicles couldn't find an acceptable gap before opposing platoon vehicles discharged completely, and most gaps appeared just before the end of green time. However, because left-turn traffic volume was low, all left-turn vehicles were able to make the turn during the limited green time and no vehicles failed to cross the intersection in these cycles. For vehicles arriving on red or at the beginning of green time, the delay is long. However, for vehicles arriving at time close to the end of green, delay is short or close to zero.

3.2.5 Summary of Input Information for Studied Lane Groups

In summary, three through lane groups and a left-turn lane group are studied in this research. Specific information for the intersections and lane groups has been described in Section 3.2.1 through Section 3.2.4. Table 3.1 shows the summary of the fixed input information used in the computations for the HCM delay model. Other parameters, such as the lane group volume and the number of vehicles arriving on green, all vary from cycle to cycle.

Table 3.1 Summary of Fixed Input Data for Studied Lane Groups

Intersection	Subject Lane Group	Cycle Length, C (sec)	Number of Lanes	Effective Green Time, g (sec)	Analysis Period, T
Wells-Grand	SB Through	75	2	31.0	75 sec (0.021 h)
LaSalle-Ohio	SB Through		3	28.7	
LaSalle-Ontario	NB Through		3	35.1	
LaSalle-Grand	NB Left-turn		1	39.7	

3.3 Field Measurement of Saturation Flow Rate at Signalized Intersection

Saturation flow rates of the studied lane groups are measured directly in the field, cycle by cycle. The method of field measurement of saturation flow rate at signalized intersections described in

Appendix H of Chapter 16, HCM 2000 is used. Time is recorded when the front axle of each vehicle crosses the stop line. The measurement starts when the front axle of the first vehicle in the queue passes the stop line and ends when the front axle of the last queued vehicle passes the stop line during the same green time. Usually, saturation flow rate is achieved after about 10 to 14 seconds of green, which corresponds to the front axle of the fourth to sixth passenger car crossing the stop line after the beginning of green. The analyst selected the fourth vehicle as the starting point to measure the saturation headways. The average headway to obtain the saturation flow rate is calculated as:

$$h = \frac{T_{last} - T_4}{(n-4)}, \text{ and} \qquad s = \frac{3600}{h} \qquad \text{Eq. (3.10)}$$

where

h = average headway (sec);

s = saturation flow rate (veh/h/ln);

T_4 = the time that the front axles of the fourth queuing vehicle crossing the stop line;

T_{last} = the time that the front axles of the last queued vehicle crossing the stop line; and

n = number of vehicles in queue.

The field measured saturation flow rate for each studied lane group in the analysis period is defined as the average of saturation flow rates measured in 48 cycles, including all normal and unusual cycles. Table 3.2 summarizes the average saturation flow rates of the studied lane groups.

Table 3.2 Summary of Average Saturation Flow Rates

Intersection	Subject Lane Group	Measured Saturation Flow Rate (veh/h/ln)	Standard Error (veh/h/ln)
Wells-Grand	SB Through	1712	33
LaSalle-Ohio	SB Through	2030	26
LaSalle-Ontario	NB Through	1603	48
LaSalle-Grand	NB Left-turn	284	17

The field-observed saturation flow rates appear to vary by lane group even among the through lane groups. The saturation flow rate of the southbound through movement at LaSalle-Ohio intersection is the highest. The saturation flow rate of the northbound left-turn movement at LaSalle-Grand intersection is significantly low due to the permissive only signal phase and the need to yield to opposing traffic.

3.4 Field Measurement of Control Delay at Intersections

Field control delay was manually measured in the field on a cycle by cycle basis. The proposed HCM 2000 field delay method described in Appendix A of Chapter 16 in the HCM 2000 was adopted. According to this method, delay is not measured directly during vehicle deceleration and acceleration. However, a reasonable estimate of control delay can be obtained using the method. A worksheet was developed for recording observations and computations of average control delay. See Appendix B for the description of field measurements.

The method requires that the range of intervals for counting the number of vehicles-in-queue to be between 10 and 20 seconds, and that the regular intervals not be an integer divisor of the cycle length. Since the cycle length is 75 seconds the analyst used 12 seconds for a count interval. The count started at the beginning of the red phase for the studied lane groups. At the locations where the video cameras were set up, signal displays for studied lane groups cannot be seen directly. For Wells-Grand intersection, queue counts started when the eastbound and westbound traffic started to move during their green phase. An error between the start time and the actual beginning of the red time for southbound movement exists, but is not significant and doesn't affect the results. For LaSalle-Ohio, LaSalle-Ontario and LaSalle-Grand intersections, the beginning of the red time was determined for the studied lane groups by observing the signal display for opposing

traffic, which is identical to that for the studied lane groups. Control delay was calculated from manual counting of queuing vehicles cycle by cycle. See Table A.1 through Table A.4 in Appendix A for manually measured delays for the studied lane groups. Table 3.3 presents the summary statistics of control delay for 48 cycles for each studied lane group.

Table 3.3 Summary of Control Delay Statistics

Intersection	**Subject Lane Group**	**Mean Control Delay** (sec/veh)	**Standard Deviation** (sec/veh)	**Standard Error** (sec/veh)
Wells-Grand	SB Through	25.55	3.47	0.50
LaSalle-Ohio	SB Through	10.63	4.95	0.71
LaSalle-Ontario	NB Through	16.22	8.48	1.22
LaSalle-Grand	NB Left-turn	23.31	13.52	1.95

CHAPTER 4. RESULTS

In this chapter, saturation flow rate and *kI*-value are estimated for each studied lane group using the HCM delay equation with default values, field calibration, and optimization, respectively. Comparisons of control delay mean square error (MSE) and corresponding parameters, saturation flow rate and *kI*, are conducted for each studied lane group. Control delay obtained from (a) field measurements, (b) the HCM control delay model using default parameter values, (c) field calibrated and (d) optimized saturation flow rate and *kI* are plotted against cycle number. The delays obtained for each cycle are grouped into preset intervals and the delay distributions are compared. Once delays have been estimated for each lane group, the appropriate level of service (LOS) for each lane group is determined on a cycle-by-cycle basis based on the LOS criteria for signalized intersections (1). Further, the distribution of LOS is analyzed to identify if the HCM control delay model reflects the real performance of these lane groups. Finally, the reliability of the HCM control delay model is evaluated. All results are analyzed in detail and possible factors contributing to the discrepancies are discussed for each studied lane group.

4.1 Summary of Saturation Flow Rate and *kI*-value of Studied Lane Groups

The adjusted saturation flow rates and *kI*-value were estimated for each studied lane group using the HCM delay equation with default values, field calibrated saturation flow, and optimization, respectively. Data for 48 cycles for each through movement and for 45 cycles for the left-turn movement were used. Table 4.1 shows the summary of the saturation flow rate and *kI*-value calculated for each lane group. The corresponding control delay MSEs are also given in the table.

These saturation flow rates and *kI*-values will be used in the HCM control delay model to obtain control delays.

Table 4.1 Summary of Saturation Flow Rates, *kI*-values and Corresponding Control Delay MSEs by Different Methods

Movement/Intersection	Calibration Method	Adjusted Saturation flow Rate (veh/h/ln)	*kI*	MSE
SB Through / Wells-Grand	HCM Default	1591	0.5	16.840
	Field Calibrated	1712	0.22	8.244
	Optimized	1900	0.5	8.146
SB Through / LaSalle-Ohio	HCM Default	1500	0.5	73.299
	Field Calibrated	2030	0.44	13.681
	Optimized	2100	0.3	13.253
NB Through / LaSalle-Ontario	HCM Default	1517	0.5	32.685
	Field Calibrated	1603	0.22	36.738
	Optimized	1550	0.5	32.225
NB Left-turn / LaSalle-Grand	Default	206	0.5	427.323
	Field Calibrated	284	0.39	158.542
	Optimized	320	0.5	151.303

From Table 4.1, it can be seen that the saturation flow rate calculated using the HCM 2000 is consistently the lowest when compared with the field calibrated and optimized values. For the southbound through lane group at LaSalle-Ohio intersection, there is a significant difference between the saturation flow rate calculated using the HCM equation with default values and that obtained using field calibration or optimization. The calibrated and optimized saturation flow rates even exceed the ideal saturation flow rate (1900 veh/h/ln) used in the HCM. However, for northbound through lane group at Ontario-LaSalle intersection, the saturation flow rate estimated using the three different methods are close, and the differences are less than 100 veh/h/ln.

As expected, the smallest control delay MSE is obtained using the optimized saturation flow rate and *kI* for all four studied lane groups. The control delay MSE calculated using field

calibrated values is quite close to that using the optimized values. However, in most cases, the MSEs are significantly high when the HCM default saturation flow rate and *kI*-value are used. Only for the southbound through lane group at LaSalle-Ontario intersection, the control delay MSE based on the HCM default values is smaller than that based on field calibrated values. It is evident that the HCM control delay model may not accurately reflect the operation of studied lane groups when the HCM default values are used.

Usually, arrivals are assumed when estimating control delay using the HCM delay model, that is, Arrival Type 3 (AT3) is used. Table 4.2 shows the control delay MSE using the HCM default saturation flow rate and *kI* with/without default arrival type. For all studied lane groups, if the proportion of vehicles arriving on green is not considered cycle by cycle, the control delay MSE increases significantly. This indicates that the consideration of arrival type or proportion of vehicles arriving on green is necessary. The default arrival type may not appropriately reflect the real conditions of the studied lane groups. The analysis of the control delay using the HCM default saturation flow rate and *kI*-value for the individual lane groups in the following sections in this chapter is based on the incorporating cycle-by-cycle proportion of vehicles arriving on green.

The tuning parameters, saturation flow rate (*s*) and *kI*, may be not calibrated simultaneously. Table 4.3 shows the control delay MSEs with field calibrated saturation flow rate and/or *kI*. When only saturation flow rate is calibrated, the default value of $kI = 0.5$ is used, and when only *kI* is calibrated, the saturation flow rate is based on the HCM equation with default values. A lower MSE is obtained when only saturation flow rate is calibrated for all studied movements.

This indicates that the calibration of saturation flow rate is more critical than the calibration of *kI*-value.

Table 4.2 Comparison of Control Delay MSE Using the HCM Default Saturation Flow Rate and *kI* with/without Default Arrival Type

Movement/ Intersection	The HCM Default	Adjusted Saturation Flow (veh/h/ln)	*kI*	AT	MSE
SB Through / Wells-Grand	*s* and *kI*	1591	0.5	-	16.840
	s, kI and AT	1591	0.5	3	34.919
SB Through / LaSalle-Ohio	*s* and *kI*	1500	0.5	-	73.299
	s, kI and AT	1500	0.5	3	268.544
NB Through / LaSalle-Ontario	*s* and *kI*	1517	0.5	-	32.685
	s, kI and AT	1517	0.5	3	73.037
NB Left-turn / LaSalle-Grand	*s* and *kI*	206	0.39	-	427.323
	s, kI and AT	206	0.5	3	742.378

Table 4.3 Comparison of Control Delay MSE with Field Calibrated Saturation Flow Rate and/or *kI*

Movement/Intersection	Field Calibration	Adjusted Saturation Flow (veh/h/ln)	*kI*	MSE
SB Through / Wells-Grand	*s* and *kI*	1712	0.22	8.244
	s only	1712	0.5	10.301
	kI only	1591	0.22	10.366
SB Through / LaSalle-Ohio	*s* and *kI*	2030	0.44	13.681
	s only	2030	0.5	13.925
	kI only	1500	0.44	68.78
NB Through / LaSalle-Ontario	*s* and *kI*	1603	0.22	36.738
	s only	1603	0.5	32.946
	kI only	1517	0.22	34.745
NB Left-turn / LaSalle-Grand	*s* and *kI*	284	0.39	158.542
	s only	284	0.5	160.343
	kI only	206	0.39	356.781

4.2 Southbound Through Lane Group at Wells-Grand Intersection

In the process of optimization, the control delay MSE varies with different combination of saturation flow rate and *kI*. Figure 4.1 shows the distribution of MSEs with a series of adjusted

saturation flow rate, *s*, and parameter, *kI*. By definition, the optimized saturation flow rate and *kI* yield the smallest MSE. The MSEs calculated using the HCM default values and field calibrated values are also plotted together in order to compare them with those calculated using optimized values.

Figure 4.1 illustrates that, for some *kI* values, there are MSE values less than 10 with corresponding saturation flow rate ranging from 1500 veh/h/ln to 2000 veh/h/ln, and there are only minor discrepancies between the MSEs for different saturation flow rate in this range. It also can be seen from the figure that the MSE obtained using field calibrated parameters is close to that estimated by the optimized parameters, and the values of the two MSEs are less than 9. That is, the average error in control delay between model estimate and field measurement is less than 3 seconds. However, the MSE calculated using the HCM default values is twice as that obtained using field calibrated or optimized saturation flow rate and *kI*. The control delay discrepancy between model estimate and field measurement is over 4 seconds.

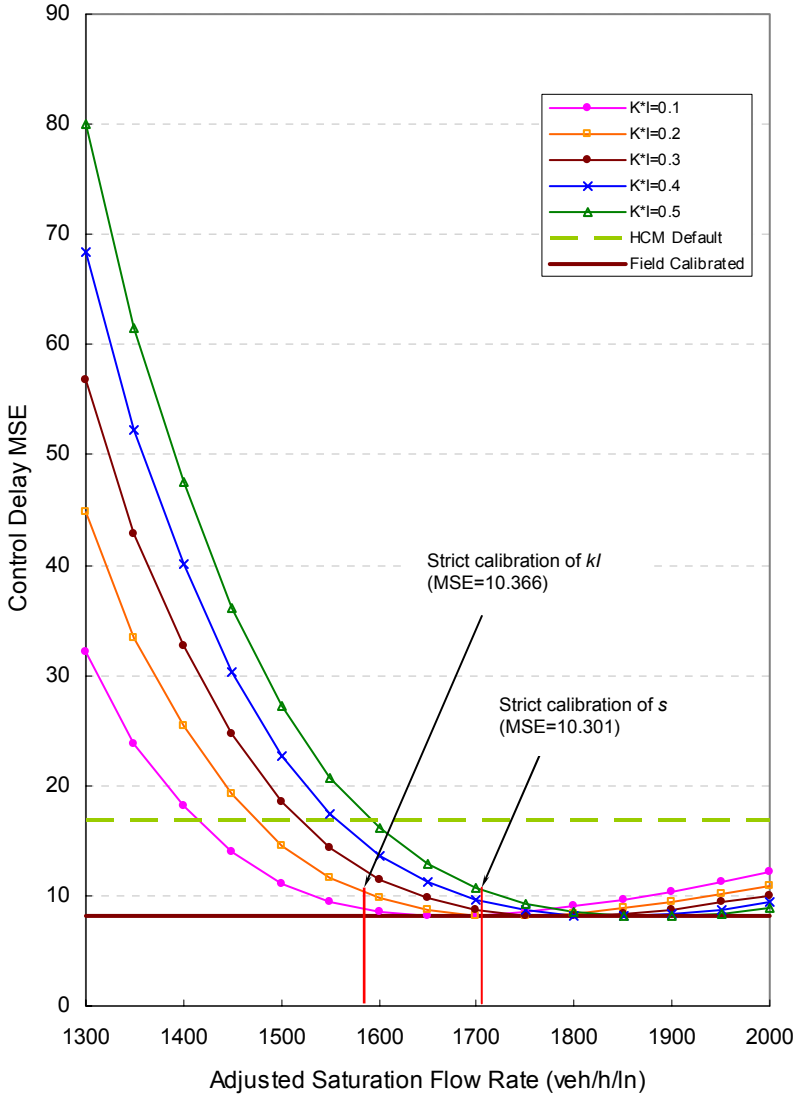

Figure 4.1 Control Delay MSE vs. Saturation Flow Rate, *s*, and Parameter, *kI,* for the Southbound Through Lane Group at Wells-Grand Intersection

Figure 4.2 shows the comparisons of control delay obtained from field measurement and HCM delay model using the HCM default, field calibrated, and optimized saturation flow rate and *kI* value cycle by cycle. In total, 48 control delays are compared. The comparisons indicate that there is a significant difference between the control delay obtained from field measurement and

the HCM model using the default values, and apparently the HCM model with default values trends to overestimate the delays. The curves of control delay obtained from the HCM model using field calibrated and optimized saturation flow rate and *kI* are almost identical. The overall shape of curves of control delay estimated using field calibrated and optimized saturation flow rates and *kI* values are similar to that from the field measurement.

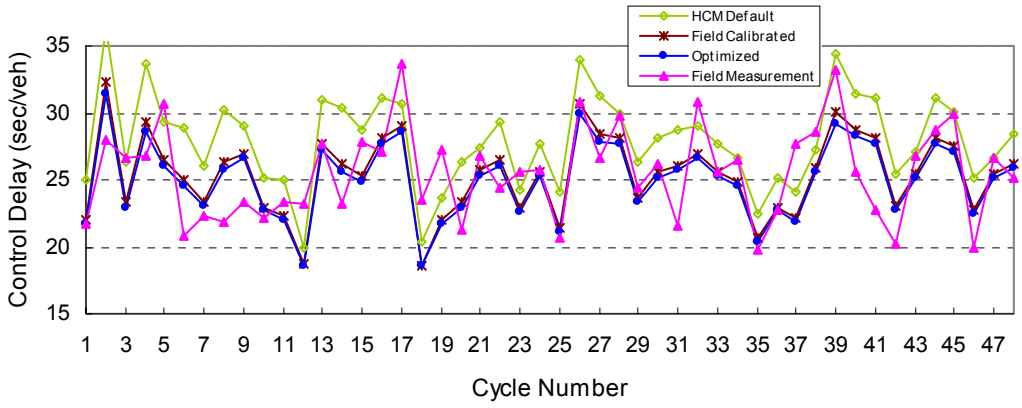

Figure 4.2 Comparisons of Control Delay for the Southbound Through Lane Group at Wells-Grand Intersection

Figure 4.3 shows the distributions of control delay obtained from the field measurement and the HCM delay model using the default, field calibrated and optimized saturation flow rates and *kI* values. Those obtained from field measurements and the HCM model using field calibrated or optimized saturation flow rate and *kI* value are quite close. However, the distribution curve of control delay obtained using the HCM default values shifts to the right, and this indicates that the control delay estimated by the HCM default values is higher than that estimated using other methods.

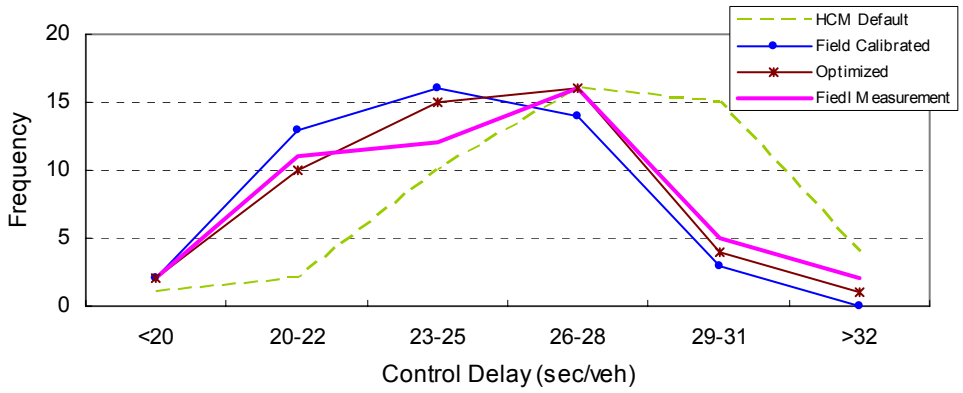

Figure 4.3 Distributions of Control Delay for the Southbound Through Lane Group at Wells-Grand Intersection

Even though there may be differences in delay estimation by the various calibration methods, it is important to test whether these will materially alter the lane group level of service (LOS). The discretization of delay to six LOS groups is therefore worth investigating.

Figure 4.4 shows the distributions of LOS determined by control delays obtained using field measurement and the HCM delay model with the HCM default, field calibrated, and optimized saturation flow rates and *kI* values. The distributions of LOS determined by control delay obtained from the field measurement and the HCM model with field calibrated and optimized saturation flow rates and *kI* values are identical. The distribution of LOS determined by the control delay estimated using the HCM model with the HCM default saturation flow rate and *kI* value is slightly different, since one LOS "D" is estimated. Overall, in 44 out of 48 cycles the HCM model predicts the same LOS as the field measurements no matter which set of saturation flow rate and *kI* are used. The distributions of level of service are approximately the same whether control delays are obtained from field measurement or the HCM model.

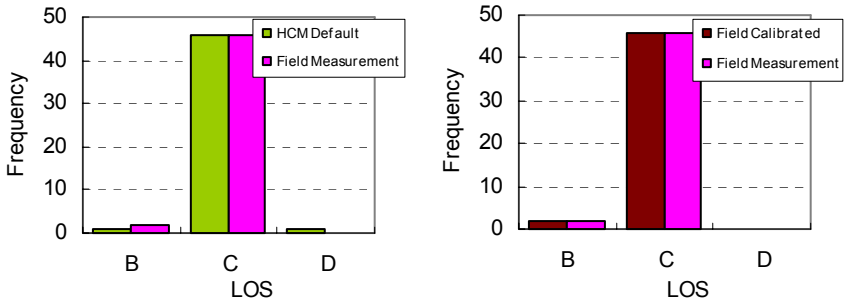

a. The HCM model using the HCM default *s* and *kI* vs. field measurement

b. The HCM model using field calibrated *s* and *kI* vs. field measurement

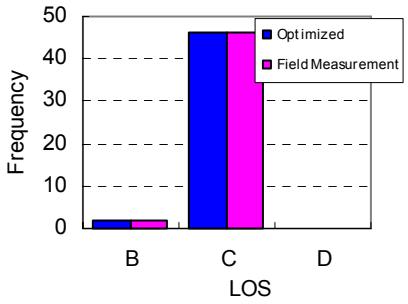

c. The HCM model using optimized *s* and *kI* vs. field measurement

Figure 4.4 Distributions of LOS for the Southbound Through Lane Group at Wells-Grand Intersection

In this research, the equation $\Pr\left(\left|d^{Model} - \overline{d}^{Field}\right| \le \delta\right) > \alpha$ (Equation 3.7) is used to identify if the HCM control delay model accurately evaluates the performance of signalized intersections. The maximum difference (δ), which is the difference between the delay estimated using the model and the average delay obtained from the field measurement, and the assurance level (α) are the critical factors determining if the delays obtained from the HCM control delay model are acceptable. For different assurance levels, the maximum difference value may vary. Forty-eight

control delays estimated using the HCM control delay model are compared with the average control delay obtained from the field measurement.

Table 4.4 shows the maximum differences at four assurance levels for the delays estimated for this lane group. As an example, one can see from the table that the HCM default-based model will be within 5.6 seconds from the measured field delay at 85% assurance level. Thus, when the HCM default saturation flow rate and *kI* value are used in the HCM delay model, the maximum difference is higher than 5 seconds for all assurance levels analyzed. The maximum difference for control delays estimated using the HCM delay model with field calibrated and the optimized saturation flow rates and *kI* values is lower than 4 seconds at the 85% assurance level. At each assurance level, the maximum differences for delays estimated using field calibrated and the optimized saturation flow rates and *kI* values are almost the same.

Table 4.4 Maximum Difference (sec) at Specified Assurance Levels for the Southbound Through Lane Group at Wells-Grand Intersection

Assurance Level, α	**90%**	**85%**	**80%**	**75%**
Using the HCM Default *s* and *kI*	5.9	5.6	5.3	5.2
Using Field Calibrated *s* and *kI*	5.0	3.8	3.5	3.2
Using Optimized *s* and *kI*	4.4	3.8	3.5	3.1

The analysis of control delay MSE and the distribution of delay and LOS indicate that the discrepancy between the results of field measurement and the HCM model using field calibrated or optimized parameter values is not significant. However, the saturation flow rate estimated using the HCM default parameter values is lower than that obtained from field calibration and optimization, and as a consequence, the control delay is overestimated. Therefore, calibrating the saturation flow rate is necessary for obtaining accurate control delays from the HCM model for this through lane group at Wells-Grand intersection. However, calibrating *kI* value may not be as

important as calibrating saturation flow rate when the saturation flow rate is between 1700veh/h/ln and 1900veh/h/ln.

4.3 Southbound Through Lane Group at LaSalle-Ohio Intersection

Figure 4.5 shows the distribution of MSEs with a series of adjusted saturation flow rate, *s*, and parameter, *kI* for this intersection. It indicates that when saturation flow rate exceeds 1800veh/h/ln, the control delay MSE approaches the minimum value for all *kI* values. However, when saturation flow rate is below 1800veh/h/ln, the corresponding MSE increases dramatically. That is, the difference of control delay between field measurement and model estimate increases significantly. Since the default HCM saturation flow rate is 1500veh/h/ln, the corresponding control delay MSE is much higher than that estimated using field calibrated or optimized saturation flow rate and *kI*. The average difference of control delay between field measurement and model estimate in these cases is over 8 seconds. On the other hand, the saturation flow rates obtained using field calibration and optimization are very close. The MSEs obtained using these two methods are almost identical and the average difference of control delay between field measurement and model estimate is no more than 4 seconds.

Figure 4.6 shows the comparisons of control delay estimated from field measurement and HCM delay model using the HCM default, field calibrated, and optimized saturation flow rates and *kI* values cycle by cycle. In total, 48 control delays are compared. In most cycles, the control delay estimated by the HCM model using default values is significantly higher than that obtained from the field measurements. This indicates that the control delay is overestimated using the HCM model with default values. The curves of the control delay estimated using the HCM model with field calibrated and optimized saturation flow rates and *kI* values are almost identical. The

overall shape of the curves of control delay obtained from field measurement and the HCM model using field calibrated and optimized saturation flow rates and *kI* values are quite similar.

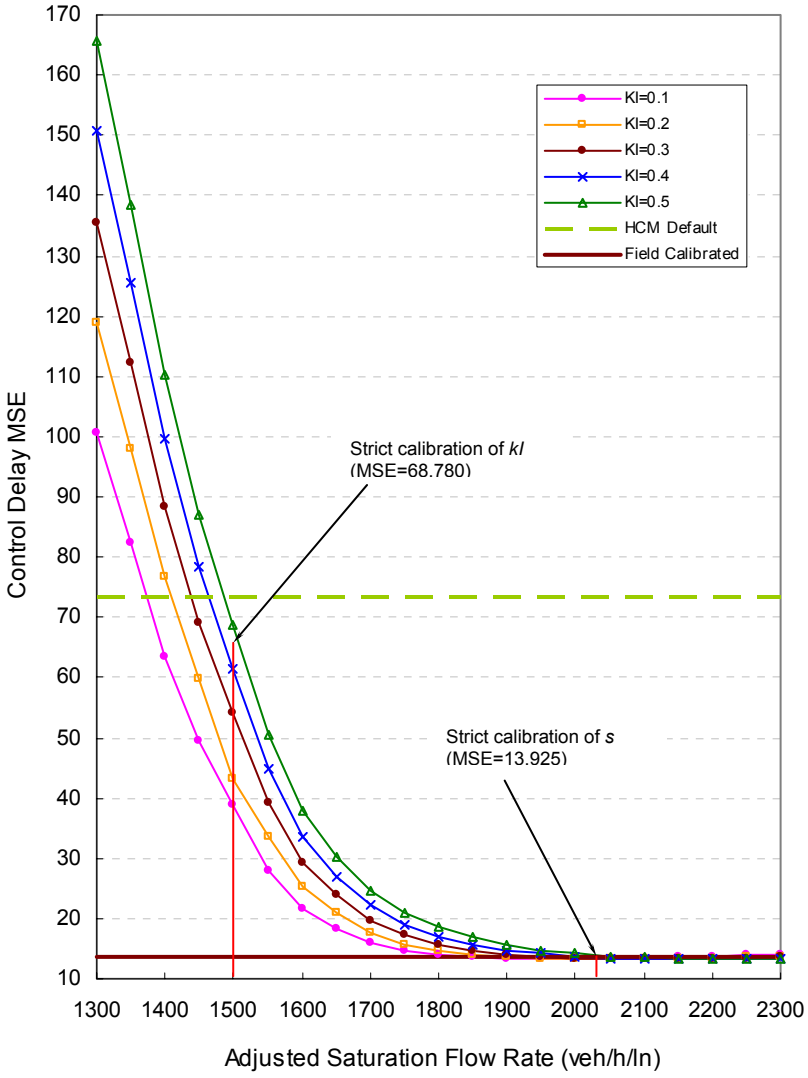

Figure 4.5 Control Delay MSE vs. Saturation Flow Rate, *s*, and Parameter, *kI,* for the Southbound Through Lane Group at LaSalle-Ohio Intersection

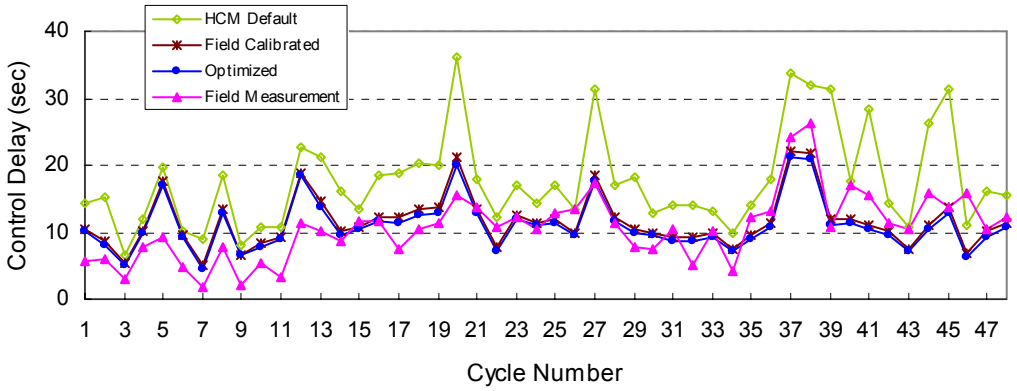

Figure 4.6 Comparison of Control Delay for the Southbound Through Lane Group at LaSalle-Ohio Intersection

Figure 4.7 shows the distributions of control delay obtained from the field measurement and the HCM delay model using various saturation flow rates and *kI* values. The distribution of delay estimated from the field measurement is a little dispersed. The distribution of control delay estimated from the HCM model using field calibrated and optimized saturation flow rates and *kI* values are similar. The distribution curve of control delay obtained from the HCM model using default values is flat and has a shift to the right. This indicates that the default HCM control delay is higher than that estimated using other methods.

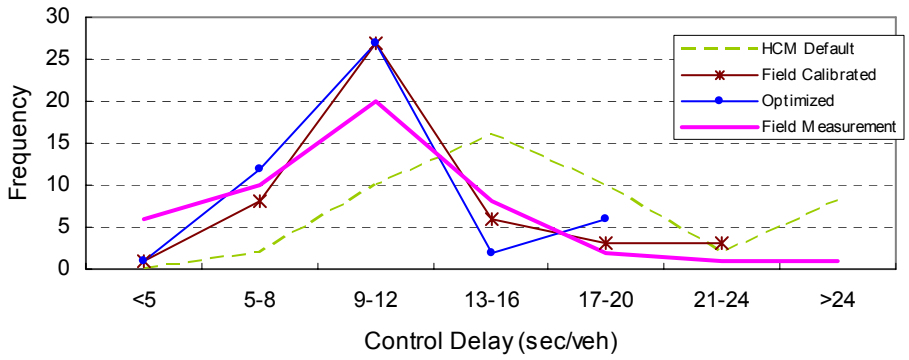

Figure 4.7 Distributions of Control Delays for the Southbound Through Lane Group at LaSalle-Ohio Intersection

Figure 4.8 shows the distributions of LOS determined by control delay obtained using the field measurement and the HCM delay model with the HCM default, field calibrated, and optimized saturation flow rates and *kI* values. More LOS "C"s and fewer LOS "A"s are estimated when using the HCM delay model with the default saturation flow rate and *kI* value, compared to that determined by field measurements. That is, the control delay obtained from the HCM model using the HCM default values overestimates field delay (or underestimates field LOS). The same conclusion is drawn from the analysis of control delay distribution in the previous discussion. The distributions of LOS estimated using the HCM delay model with field calibrated and optimized saturation flow rates and *kI* values are similar to those obtained using field measurements. Overall, in 26, 33, and 35 out of 48 cycles, the LOSs estimated using the HCM delay model with default, field calibrated and optimized saturation flow rates and *kI* values, respectively, are identical to those obtained from field measurements.

Table 4.5 shows the maximum differences at four assurance levels for the delays estimated for this lane group. When the HCM default saturation flow rate and *kI* value are used in the HCM delay model, the maximum difference is over 9 seconds even at the 75% assurance level. The control delays estimated using this method cannot accurately reflect the situations of this lane group. However, at the 80% assurance level, the maximum difference is less than 4 seconds for control delays obtained from the HCM model with field calibrated and optimized saturation flow rates and *kI* values. The maximum difference less than 4 seconds is considered acceptable.

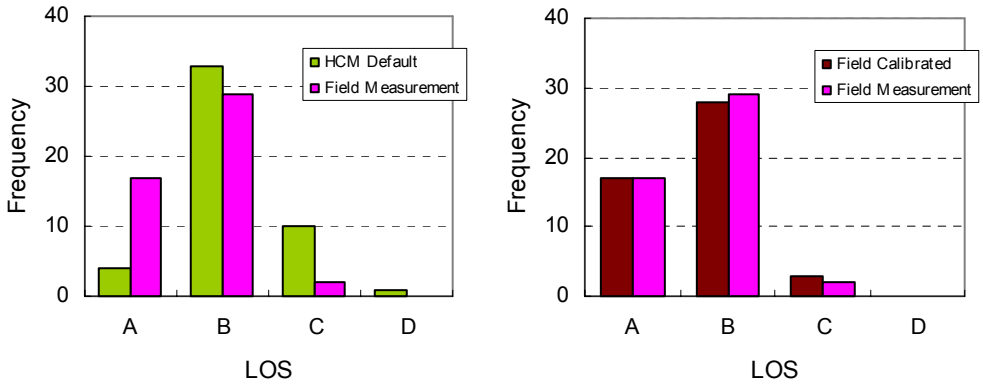

a. The HCM model using the HCM default *s* and *kI* vs. field measurement

b. The HCM model using field calibrated *s* and *kI* vs. field measurement

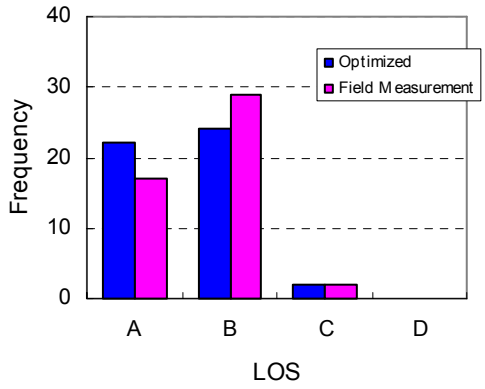

c. The HCM model using optimized *s* and *kI* vs. field measurement

Figure 4.8 Distribution of LOS for the Southbound Through Lane Group at LaSalle-Ohio Intersection

Table 4.5 Maximum Difference (sec) at Specified Assurance Levels for the Southbound Through Lane Group at LaSalle-Ohio Intersection

Assurance Level, α	**90%**	**85%**	**80%**	**75%**
Using the HCM Default *s* and *kI*	20.7	15.5	9.5	9.2
Using Field Calibrated *s* and *kI*	8.0	5.3	3.9	3.1
Using Optimized *s* and *kI*	6.6	5.5	3.6	3.4

For this lane group, the field calibrated and optimized saturation flow rates are 2030veh/h/ln and 2100veh/h/ln, respectively. They are close and much higher than that estimated using the HCM default values. They are even higher than the HCM ideal saturation flow rate. Using these two saturation flow rate, the control delays from the model are approximately the same, and the control delay MSEs, distributions of control delay and LOS are similar. If a 4-second maximum difference is acceptable at an 80% assurance level, the HCM control delay model is reliable when field calibrated or optimized saturation flow rate are used. However, the saturation flow rate estimated using the HCM default values is significantly lower than that obtained from field calibration and optimization, and apparently, the control delay are overestimated in most cycles.

The characteristics of the operation for this lane group may explain the results discussed above. The southbound through movement at LaSalle St. has good signal progression. Most vehicles in the platoon coming from the upstream intersection arrived during the green phase. This implies that vehicles joining the back of queue didn't have to stop completely. Meanwhile, neither the intersection nor the downstream lane was blocked, and the discharge speed was higher than that in stop-go situation or when congestion existed in downstream lanes.

Also, when saturation flow rate is higher than 1900 veh/h/ln, the *kI* value doesn't have much impact on the control delay result. Therefore, in this situation, only the calibration of saturation flow rate is important for estimating accurate control delays using the HCM model.

4.4 Northbound Through Lane Group at LaSalle-Ontario Intersection

Figure 4.9 shows the distribution of MSEs with a series of adjusted saturation flow rate, *s*, and parameter, *kI* for this intersection, and it indicates that the control delay MSE is sensitive to saturation flow rate and *kI*-value. A Larger *kI* value produces a smaller MSE when saturation

flow rate approaches the optimized value. For various *kI* values, the smallest MSE value appears when the saturation flow rate is within the range of 1400veh/h/ln through 1600veh/h/ln. The saturation flow rates estimated using the HCM default values and field calibration are also approximately within this range and the MSEs obtained using these two methods are close to the optimized value. Since the same *kI* value, which is equal to 0.5, is used when control delay is estimated using the HCM default values and optimized values, the MSEs obtained are almost the same. However, the field calibrated *kI* value appears to be low and as a consequence, the control delay MSE is slightly high. Compared to the previous two studied through lane groups, the average difference of control delay between model estimate and field measurement for this lane group (around 6 seconds) is higher no matter which values of saturation flow rate and *kI* are used. Figure 4.10 shows the comparisons of control delay obtained from the field measurement and the HCM delay model using different saturation flow rates and *kI* values cycle by cycle. In total, 48 control delays are compared. The curves of control delay estimated using the HCM delay model are almost the same, no matter the HCM default, field calibrated or optimized saturation flow rate and *kI* value are used. The shape of the control delay curve obtained from the field measurements is similar to those of the delay estimated by the HCM model for the first 28 cycles during the analysis period, but not for subsequent cycles. In most of the last 20 cycles, vehicles experienced longer delay due to downstream queue. The control delays based on the HCM delay model may be underestimated.

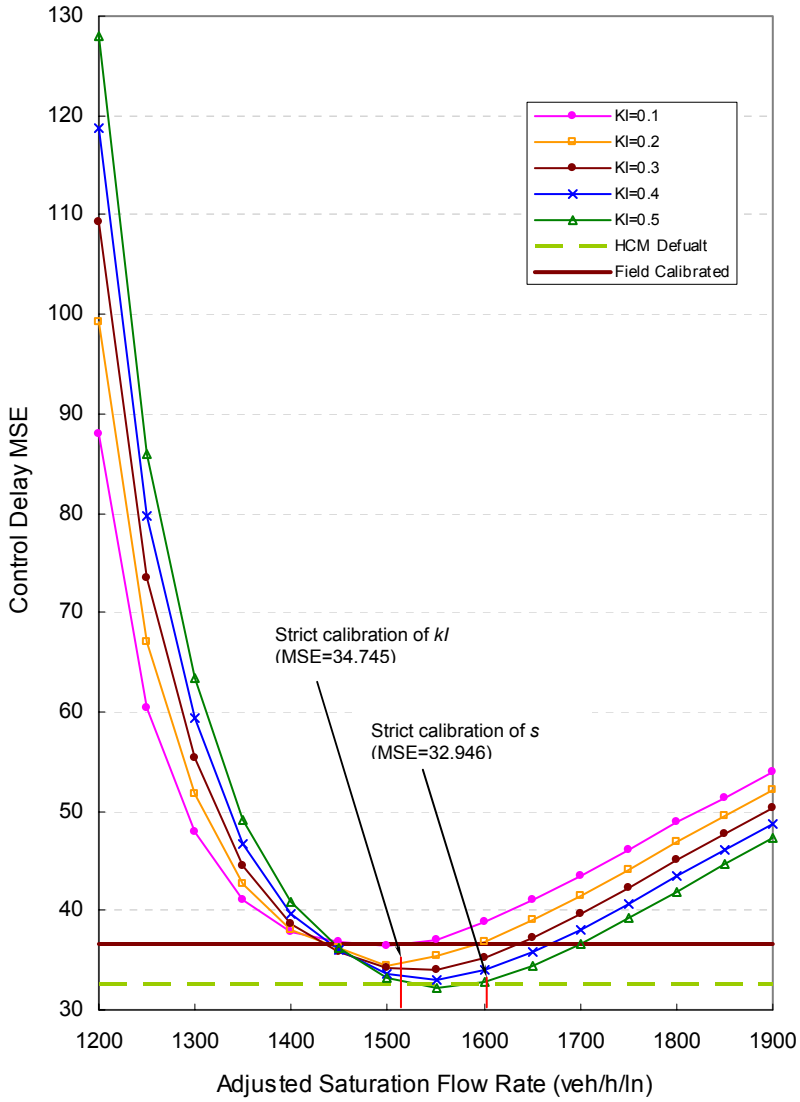

Figure 4.9 Control Delay MSE vs. Saturation Flow Rate, *s*, and Parameter, *kI,* for the Northbound Through Lane Group at LaSalle-Ontario Intersection

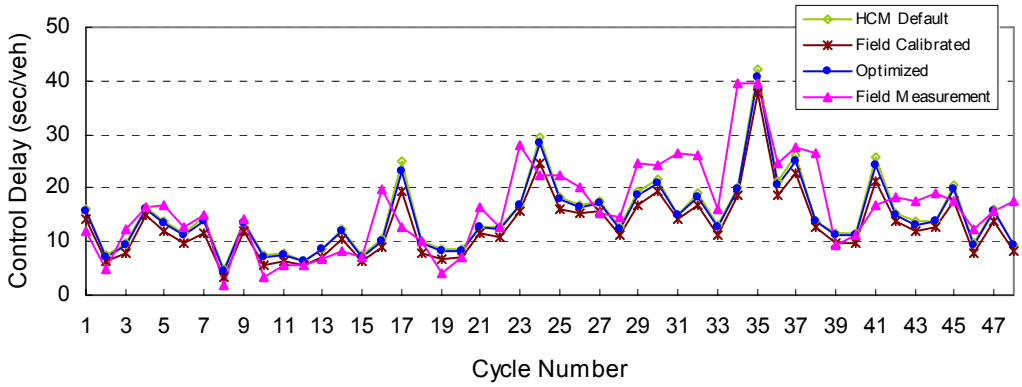

Figure 4.10 Comparisons of Control Delay for the Northbound Through Lane Group at LaSalle-Ontario Intersection

Figure 4.11 shows the distributions of control delay obtained from the field measurement and the HCM delay model with different saturation flow rates and *kI* values. The shapes of distribution curves of the model estimated control delay using the HCM default and optimized saturation flow rates and *kI* values are almost the same. The distribution curve of the field measured control delay is flatter than the three others. The distribution curve of control delay estimated using the HCM model with field calibrated saturation flow rate and *kI* value slightly shifts to the left, and this indicates the control delay may be slightly underestimated.

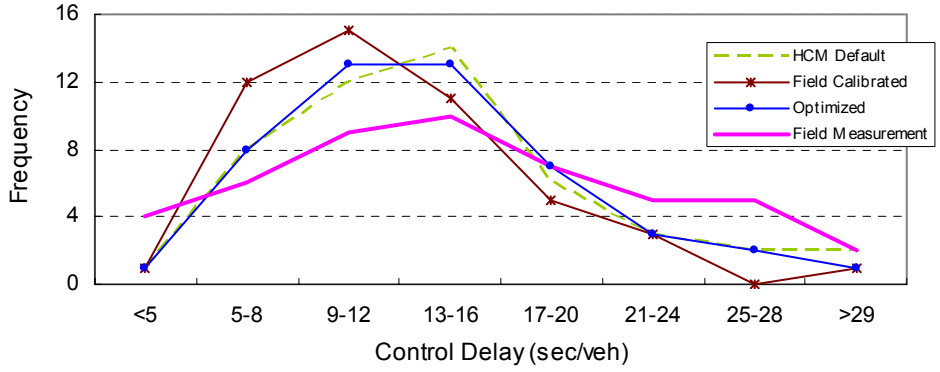

Figure 4.11 Distributions of Control Delay for the Northbound Through Lane Group at LaSalle-Ontario Intersection

Figure 4.12 shows the distributions of LOS determined by control delay obtained using the field measurements and the HCM delay model with the HCM default, field calibrated, and optimized saturation flow rates and *kI* values. More LOS "A"s and LOS "B"s are estimated when the LOS is determined using the HCM delay model compared to that determined using field measurements. This indicates that the HCM control delay model overestimates the performance of this lane group. Overall, in 31, 29 and 32 out of 48 cycles, the LOSs estimated using the HCM default, field calibrated, and optimized saturation flow rates and *kI* values, respectively, are identical to those determined using the field measured control delays.

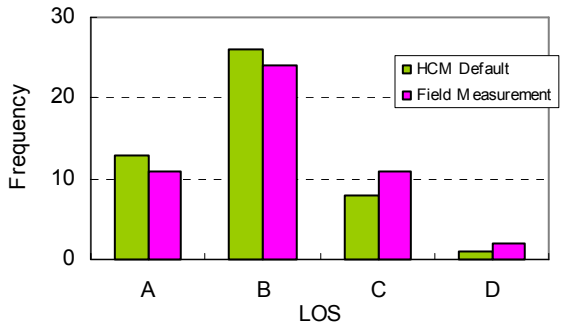

a. The HCM model using the HCM default *s* and *kI* vs. field measurement

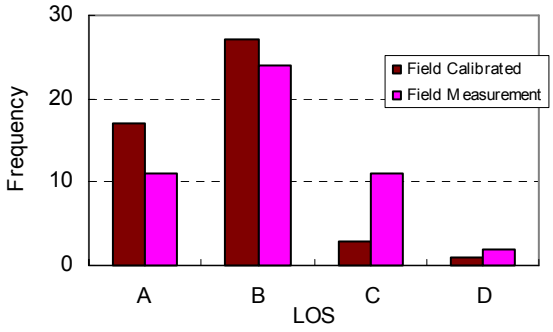

b. The HCM model using field calibrated *s* and *kI* vs. field measurement

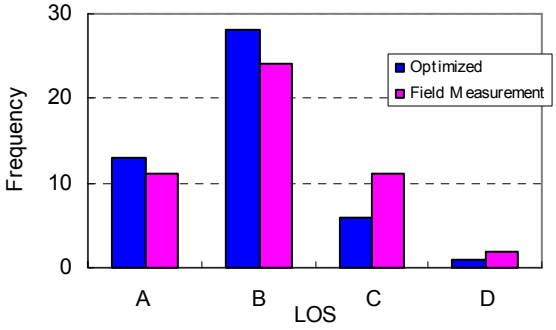

c. The HCM model using optimized *s* and *kI* vs. field measurement

Figure 4.12 Distribution of LOS for the Northbound Through Lane Group at LaSalle-Ontario Intersection

Table 4.6 shows the maximum differences at four assurance levels for the delays estimated for this lane group. At each assurance level analyzed, the maximum differences are approximately the same for the control delays estimated from the HCM model no matter which values of the saturation flow rate and *kI* are used in the model. Also, all maximum difference values calculated for this lane group are high, and even at the 75% assurance level, the maximum difference is around 8 seconds. The results shown in the table indicate that the HCM delay model may not accurately evaluate the performance of this lane group.

Table 4.6 Maximum Difference (sec) at Specified Assurance Levels for the Northbound Through Lane Group at LaSalle-Ontario Intersection

Assurance Level, α	90%	85%	80%	75%
Using the HCM Default *s* and *kI*	9.6	8.8	8.6	7.7
Using Field Calibrated *s* and *kI*	10.1	9.5	8.6	8.3
Using Optimized *s* and *kI*	9.1	8.9	8.1	7.8

For this lane group, the control delay MSEs are similar whether the HCM default, field calibrated or optimized saturation flow rate and *kI* are input into the model to estimate the delays. However, errors are slightly higher than those observed in the two previous lane groups studied. Similarly, the distributions of control delays obtained from the HCM model using the HCM default, field calibrated and optimized values are approximately the same, but are still different from the field delays. The distributions of LOS have the same characteristics. System bias of the model may cause the similarity and difference discussed above.

As described in Section 3.2, a downstream queue reduced the intersection discharge in some cycles causing extra delay. Although this delay can be measured directly from the field, the model cannot take it into consideration. A downstream queue was observed in only two cycles (cycles 16 and 23) among the first 28 cycles during the study period. However, among the last 20 cycles, vehicles experienced extra delay due to the downstream queue in 14 cycles. Due to the

difference of frequency of downstream queue, the one-hour was divided into two periods, cycles 1 through 28 and cycles 29 through 48, each having its own saturation flow.

Table 4.7 shows the control delay MSEs and the corresponding saturation flow rates and *kI* values for the two study periods. The saturation flow rate estimated using the HCM default values for each study period was kept unchanged, because it doesn't take into account the effect of a downstream queue. However, the field calibrated saturation flow rate for cycles 29 through 48 was found to be much lower than that for cycles 1 through 28 due to the effect of downstream queue. The optimized saturation flow rate also changes, and the average saturation flow rate for cycles 29 through 48 was found to be lower than that for cycles 1 through 28 although not significantly.

Table 4.7 The Optimal MSEs and Corresponding Saturation Flow Rates (veh/h/ln) and *kI* Values for the Two Study Periods at LaSalle-Ontario Intersection

	Cycles 1 - 28			Cycles 29 - 48		
Method	***s***	***kI***	**MSE**	***s***	***kI***	**MSE**
HCM Defaults	1517	0.5	20.06	1517	0.5	50.36
Field Calibrated	1742	0.17	20.34	1416	0.26	52.74
Optimized	1650	0.5	16.29	1500	0.5	49.93

For the first study period, the control delay MSEs are significantly lower than those for the total 48 cycles discussed previously, especially when the optimized saturation flow rate is used. However, the control delay MSEs for the second study period are much higher. The distributions of control delay for both study periods are plotted together in Figure 4.13. It can be seen from this figure that the delays estimated using the HCM model are approximately similar to that obtained from field measurement in cycles 1 through 28. It is obvious that if cycles 16 and 23 (during which a downstream queue occurred and the difference between delays obtained from the

HCM model and field measurement are over 10 seconds) are not considered, the MSEs for cycles 1 through 28 may be even smaller. It can be seen from the above analysis that, for cycles 1 through 28, the HCM delay model is reliable when optimized saturation flow rate and *kI* are used, but may not be reliable when the HCM defaults values and field calibrated values are used due to the higher MSE generated.

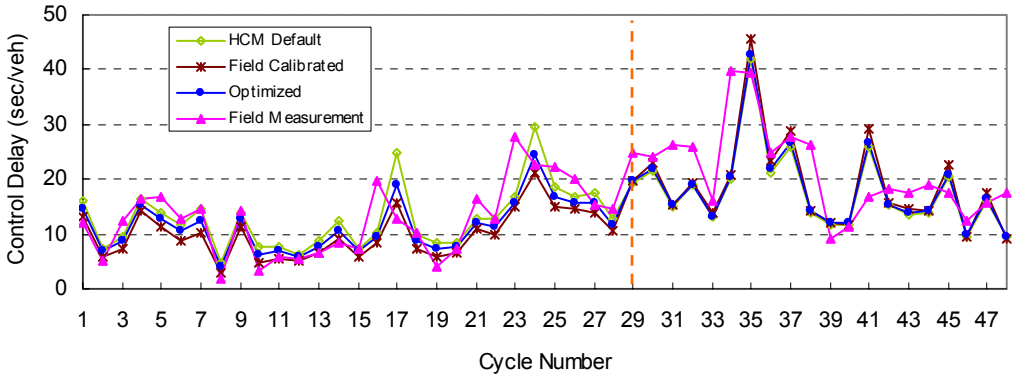

Figure 4.13 Distributions of Control Delay for the Northbound Through Lane Group with Different Saturation Flow Rates at LaSalle-Ontario Intersection

For cycles 29 through 48, the control delay MSEs are much higher than those calculated for the total 48 cycles. The smallest MSE is around 50 regardless of which saturation flow rate value is used. Figure 4.13 shows that, for these cycles, the control delays estimated using the HCM model are apparently different from those obtained from the field measurements. A possible reason that caused the difference is that downstream queue blocked the intersection in some cycles and as the result, control delay increased in these cycles. However, this effect cannot be reflected in the HCM model, although the fact is that, when the intersection is blocked by downstream queue, vehicles arriving on green have to experience more delay as if they had arrived on red.

A sensitivity analysis of the control delay MSE for cycles 29 through 48 is conducted considering vehicles arriving on green as arriving on red when the intersection is blocked by a downstream queue. Based on this consideration, the "adjusted" proportion of vehicles arriving on green is less than the "real" proportion of vehicles arriving on green. In this sensitivity analysis, the MSE is calculated for each 10% of reduction in the "real" proportion of vehicles arriving on green. Table 4.8 summarizes the sensitivity analysis results and Figure 4.14 graphically illustrates the change of the MSEs due to the reductions in the proportion of vehicles arriving on green. With a 40% of reduction in the proportion of vehicles arriving on green, the MSE for control delay estimated using optimized saturation flow rate and *kI* is the closest to that for the delay obtained from the field measurement. The value of this MSE for control delay estimated using optimized saturation flow rate and *kI* is below 30, which is significantly lower than that calculated based on the "real" proportion of vehicles arriving on green.

Table 4.8 Summary of Sensitivity Analysis for the Control Delay MSE for Cycles 29 through 48 at LaSalle-Ontario Intersection

Reduction in Proportion of Arrivals on green*	The HCM Default	Field Calibrated	Optimized		
	MSE	MSE	MSE	kI	Saturation Flow Rate (veh/h/ln)
0%	50.36	52.74	49.93	0.5	1500
10%	46.96	45.07	41.36	0.5	1550
20%	**46.88**	43.06	37.23	0.5	1550
30%	47.14	**40.84**	31.60	0.5	1600
40%	53.98	44.99	**29.65**	**0.1**	**1600**
50%	77.26	64.69	39.86	0.1	1700

* Reduction is applied to "*P*" in each cycle.

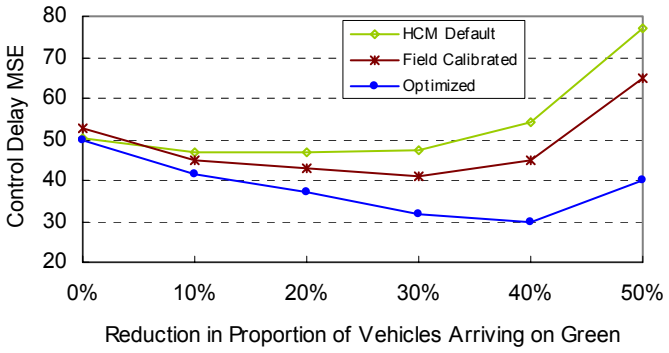

Figure 4.14 Sensitivity Analysis of the Control Delay MSEs vs. Decrease of Proportion of Arriving on Green for Cycles 29 through 48 at LaSalle-Ontario Intersection

The sensitivity analysis indicates that, if a downstream queue is present, an adjustment to the proportion of vehicle arriving on green may be necessary. In this case, the HCM model may evaluate the lane group's performance more accurately. Therefore, the presence of a queue causes a reduction in both the saturation flow rate, and the proportion of vehicles arriving on green.

4.5 Northbound Permissive Left-turn Lane Group at LaSalle-Grand Intersection

Figure 4.15 shows the distribution of MSEs with a series of adjusted saturation flow rate, *s*, and parameter, *kI* for this intersection. It can be seen from this figure that the smallest control delay MSE value for this left-turn lane group is significantly higher in comparison to that for the studied through lane groups even when an optimized saturation flow rate is used. For *kI* values of 0.1, 0.2 and 0.3, the control delay MSEs are relatively low when the corresponding saturation flow rate is in the range of 260veh/h/ln through 360veh/h/ln. The average difference of control delay between field measurement and model estimate is above 12 seconds. The saturation flow rate estimated for this lane group using the HCM default values is quite low in comparison to that

obtained using field calibration and optimization. As a result, the control delay MSE is high. The significant difference of control delay between the field measurement and the model estimate indicates that the HCM control delay model may not be accurately reflect the operation of the permissive left-turn lane groups.

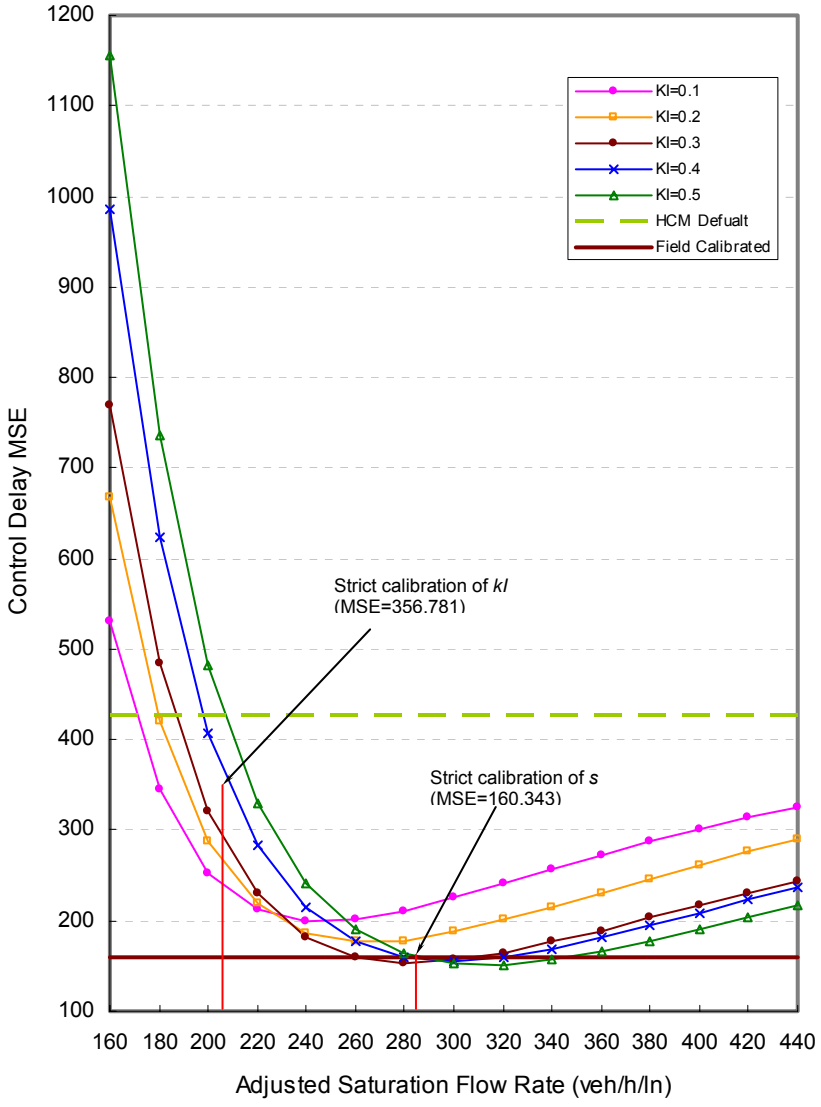

Figure 4.15 Control Delay MSE vs. Saturation Flow Rate, *s*, and Parameter, *kI,* for the Northbound Permissive Left-turn Lane Group at LaSalle-Grand Intersection

Figure 4.16 shows the comparisons of control delay obtained from the field measurement and the HCM delay model using different saturation flow rates and *kI* values on a cycle by cycle basis. In total, 45 control delays are compared. Control delays estimated using the HCM model with default values are significantly higher compared to those obtained from field measurements. The control delays estimated by the field calibrated and optimized saturation flow rates and *kI* values are similar. However, for most cycles, the delay estimated using the HCM delay model is apparently different from that obtained from the field measurement.

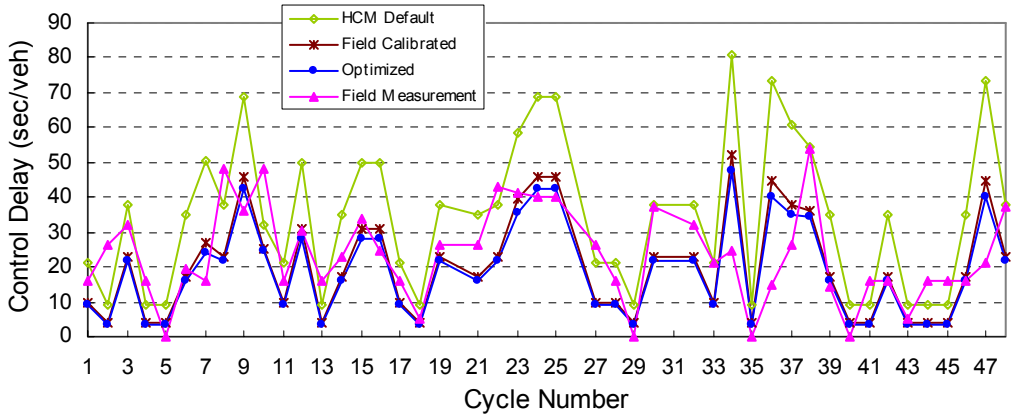

Figure 4.16 Comparisons of Control Delay for the Northbound Permissive Left-turn Lane Group at LaSalle-Grand Intersection

Figure 4.17 shows the distributions of control delay obtained by different methods. It can be seen from the figure that all the control delay distributions are very dispersed. No common characteristics can be found in the distributions of control delay, except that the distributions of control delay estimated using the HCM model with field calibrated and optimized saturation flow rates and *kI* values are approximately close.

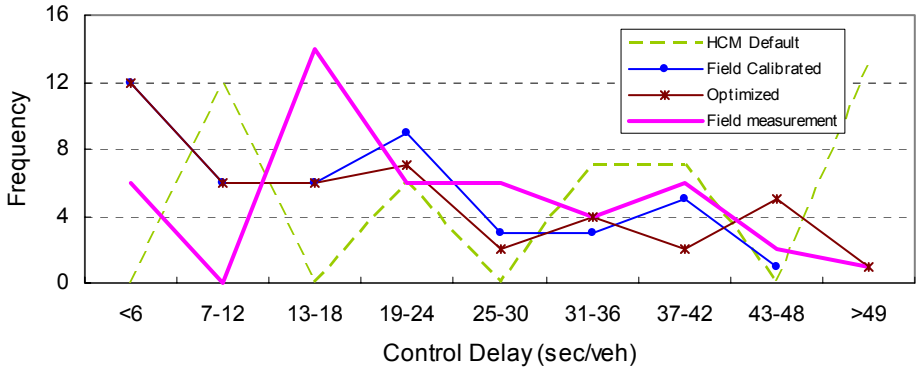

Figure 4.17 Distributions of Control Delay for the Northbound Permissive Left-turn Lane Group at LaSalle-Grand Intersection

Figure 4.18 shows the distributions of LOS determined by control delay obtained using field measurements and the HCM delay model with the HCM default, field calibrated, and optimized saturation flow rates and *kI* values. The distribution of LOS estimated by the HCM default values is quite dispersed, and this method is the only one that predicts a LOS E (in 8 out of 48 cycles). It can be seen that the HCM delay model with the default values substantially underestimates LOS. The LOS estimated using the HCM model with field calibrated and optimized saturation flow rates and *kI* values appears to produce lower delays than those obtained from field measurements. Specifically, more LOS "A"s are estimated when control delay is estimated using the HCM model than using the field measurements. Overall, in 13, 21, and 21 out of 48 cycles, the LOSs estimated using the HCM default, field calibrated, and optimized saturation flow rates and *kI* values, respectively, are identical to those determined using the field measured control delays. The distribution of LOS estimated using the HCM control delay model is not comparable with that obtained from field measurements.

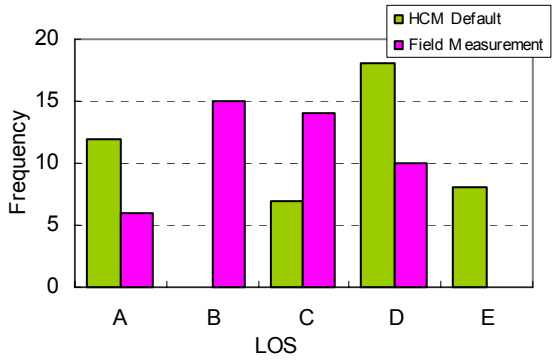

a. The HCM model using the HCM default *s* and *kI* vs. field measurement

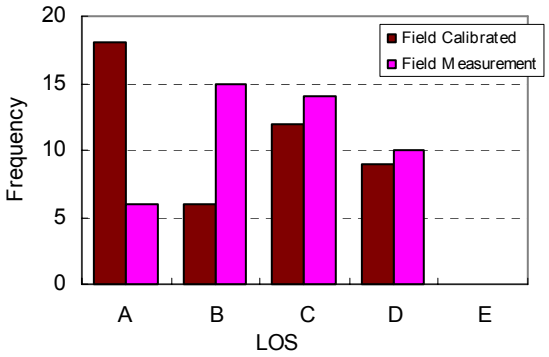

b. The HCM model using field calibrated *s* and *kI* vs. field measurement

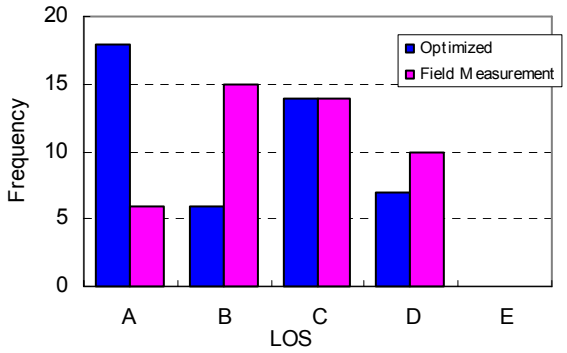

c. The HCM model using optimized *s* and *kI* vs. field measurement

Figure 4.18 Distributions of LOS for the Northbound Permissive Left-turn Lane Group at LaSalle-Grand Intersection

Table 4.9 summarizes the maximum differences at four assurance levels for the delays estimated for this lane group. The maximum difference values are significantly high for the delays obtained from the HCM model, especially when the HCM default saturation flow rate and *kI* value are used in the model to estimate the delays. That is, the control delay estimated using the HCM model is quite different from that obtained from field measurements. It is obvious that the HCM control delay model doesn't accurately reflect the operation of this permissive left-turn lane group.

Table 4.9 Maximum Difference (sec) at Specified Assurance Levels for the Northbound Permissive Left-turn Lane Group at LaSalle-Ontario Intersection

Assurance Level, α	90%	85%	80%	75%
Using the HCM Default *s* and *kI*	45.7	35.2	27	14.5
Using Field Calibrated *s* and *kI*	21.4	19.5	16.5	14.4
Using Optimized *s* and *kI*	23	19.1	15.8	12.1

The large value of control delay MSE between the HCM model and field measurement indicate that the HCM model that uses a fixed saturation flow rate for all cycles doesn't accurately estimate the delays for this permissive left-turn lane group. For permissive left-turn movement, the saturation flow rate not only depends on the conditions of its approach (e.g. lane width, approach grade, etc.), but also on the flow rate of the opposing movement. That is, the left-turn vehicles have to wait until the opposing vehicles clear the intersection during the green phase before they can find an acceptable gap to make the turn. Opposing traffic volume varies from cycle to cycle, and the time needed for opposing vehicles to clear the intersection also varies in each cycle. As a consequence, the left-turn lane group saturation flow rate could change from cycle to cycle. However, a constant value of the saturation flow rate is used in the HCM delay model to estimate average delay for each cycle, and that causes a large discrepancy between the delays obtained from the HCM model and field measurement.

Control delay estimated based on the individual saturation flow rate and the corresponding MSEs are analyzed for each cycle. Since the left-turn volume for each individual cycle is low and there are cycles in which only one left-turn vehicle is present, it is not possible to measure the saturation flow rate for each cycle in the field. As a result, neither field calibrated nor optimized saturation flow rates can be estimated. Only the saturation flow rate based on the HCM default values can be computed for each cycle. The cycle-by-cycle saturation flow rate and the resulting control delay estimated using the HCM model are listed in Table D.1 in Appendix D. Figure 4.19

shows a comparison between control delays obtained from field measurements and the HCM model using individual saturation flow rate for each cycle. It can be seen from the figure that the control delay estimated using the HCM model is still higher than that obtained from field measurement for most cycles. Therefore, it is evident that the saturation flow rate is underestimated in the HCM delay model.

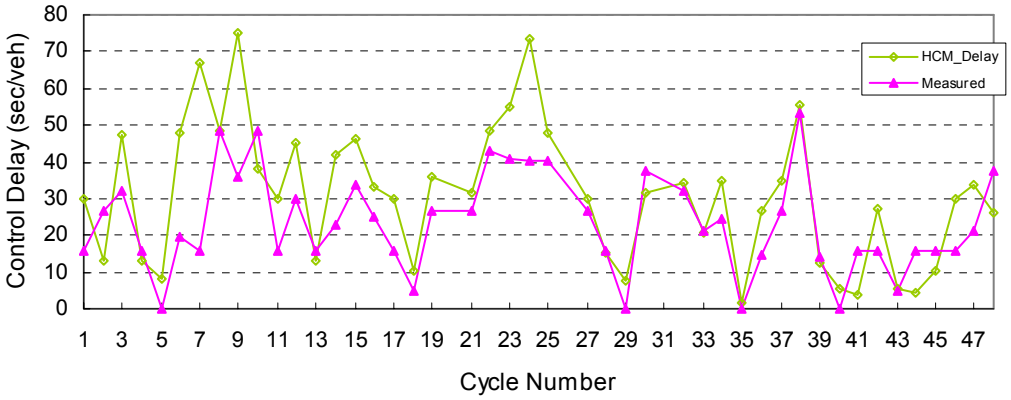

Figure 4.19 Comparison of Control Delays Obtained from the HCM Model with Cycle-by-cycle Saturation Flow Rate against Field Measurement

Nevertheless, in this case, MSE is 220 which is significantly smaller than that estimated using the fixed saturation flow rate for all cycles (at 427), still quite large in comparison to the through lane groups values. Possible reasons for this discrepancy need to be analyzed. Compared to the traffic volume for the through lane groups, the volume for the left-turn lane group is significantly lower. For the 48 cycles study period, a total of 106 left-turn vehicles were counted, that is, an average of 2-3 left-turn vehicles arrived at intersection per cycle. Because the sample size for left-turn volumes is low and the delay obtained from the field measurement is stochastic, the control delay estimated using the HCM model may be different from that obtained from field measurements. The following example helps to explain that effect. Table 4.10 shows a comparison of control

delay obtained from the HCM model and the field measurement for cycles 18 and 45. In both cycles, only one vehicle arrived at the intersection and the vehicle arrived on green. The calculation results indicate that the control delays estimated from the HCM model for these two cycles are about the same. However, the field control delays for the two cycles are significantly different. The reason is that, during cycle 18, the vehicle arrived at the end of the green phase when the opposing queue had cleared and this vehicle made the left-turn without waiting for a long gap to appear; however, during cycle 45, the vehicle arrived at the beginning of the green phase, and in order to make the left-turn, waited until the opposing queue completely discharged.

Table 4.10 Comparison of Control Delay for Cycle 18 and Cycle 45

Cycle	**Vehicles per Cycle**	**% Arriving on Green**	**Saturation Flow Rate** (veh/h/ln)	**The HCM based Control Delay** (sec/veh)	**Measured Control Delay** (sec/veh)
18	1	100.0%	191	10.5	5.0
45	1	100.0%	193	10.3	15.8

Therefore, it is difficult to determine which delay value better represents the average control delay for the cycles during which the number of arriving vehicles is low. However, the situation for through lane groups is different. For through lane groups studied, an average of more than 20 vehicles arrived during each cycle. Therefore, the average control delays obtained from the HCM model and field measurement are more comparable, and one can be more confident about these results.

In order to obtain more left-turn vehicles in one data set, control delay in each 5-minute (a total of 12 groups of control delays in one hour) is analyzed. Table 4.11 shows the control delay estimated using the HCM model and from the field measurement as well as the adjustment factor for left turns in lane group for reference purpose. The difference of control delay between model estimate and field measurement is small when the number of left-turn vehicles and/or opposing

vehicles are low, but when both of them are high, the difference increases significantly (see Groups 2, 3, and 6). The HCM model overestimates the control delay. In the HCM control delay model, the higher opposing flow causes a much lower adjustment factor for left turns. As a consequence, the saturation flow rate for left-turn lane group decreases and unmet demand is present. However, the field observation indicates that left-turn vehicles always try to find an opportunity even on the last second yellow time or all red time to accomplish their turning movement.

Table 4.11 Comparison of Control Delay Using 5-minute Data for the Northbound Permissive Left-turn

Group	No. of NB Left-turn Vehicles	No. of Opposing vehicles	f_{LT}	Control Delay (sec/veh)	
				The HCM Based	Field Measured
1	6	137	0.123	31.1	23.0
2	10	145	0.118	131.1	21.8
3	10	132	0.137	76.2	31.5
4	10	118	0.164	36.5	26.1
5	5	140	0.114	24.4	18.0
6	12	126	0.155	86.4	37.4
7	8	110	0.184	24.0	30.7
8	5	106	0.180	16.8	27.8
9	13	92	0.240	26.0	18.4
10	10	98	0.211	24.5	25.6
11	6	107	0.186	11.8	14.0
12	11	99	0.209	24.2	22.2

4.6 Overall Summary

In order to assess the accuracy of the HCM control delay model, regression analyses are conducted for the combined 144 control delay observations for through lane groups and 45 control delay observations for the permissive left-turn lane group estimated using the HCM model.

- Through Lane Group

Figures 4.20 shows the field measured control delays against estimated HCM control delays using the HCM default, field calibrated, and optimized saturation flow rates and *kI* values, respectively, for the through lane groups. In these figures, the solid line is the regression line, which reflects the real relationship between the control delay estimated using the HCM model and field measurements. The dotted line represents the ideal relationship, that is, when the control delay estimated using the HCM delay model equals to field measured control delay.

Figure 4.20a shows that the control delays estimated by the HCM default values are scattered and the R^2 value is low. These estimated delays may not reflect the real performance of the through lane groups. In most of cases, the control delays are overestimated, especially when their values are low. However, Figure 4.20b and 4.20c show that the control delays estimated using the HCM model with field calibrated and optimized saturation flow rates and *kI* values, respectively, are close to the regression line. For these cases, the R^2 values are high and quite similar. These indicate that the HCM control model with field calibrated and optimized saturation flow rates and *kI* values are reliable to evaluate the performance of the through lane groups. Figures 4.20b and 4.20c also illustrate that when actual control delay increases in the field, the model based control delay estimated using these two methods may be underestimated.

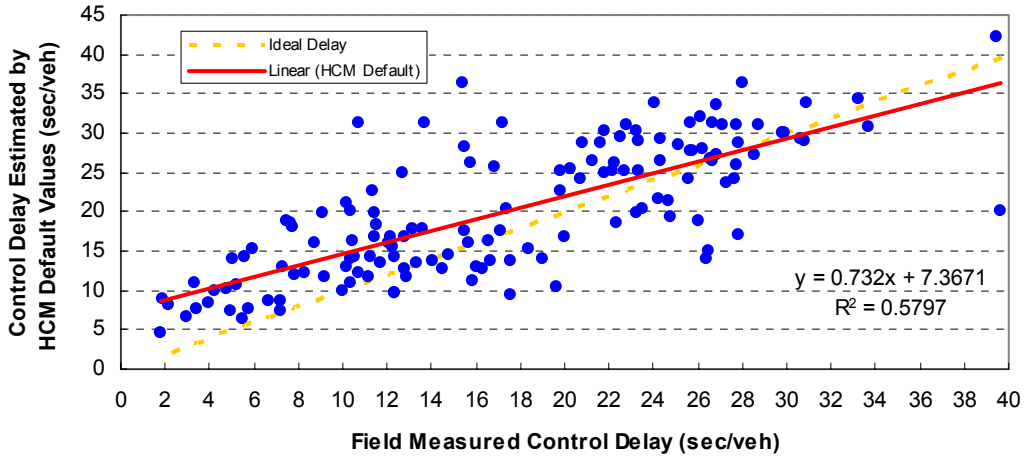

a) Comparison of control delay estimated using the HCM model with the HCM default values to the field measurements

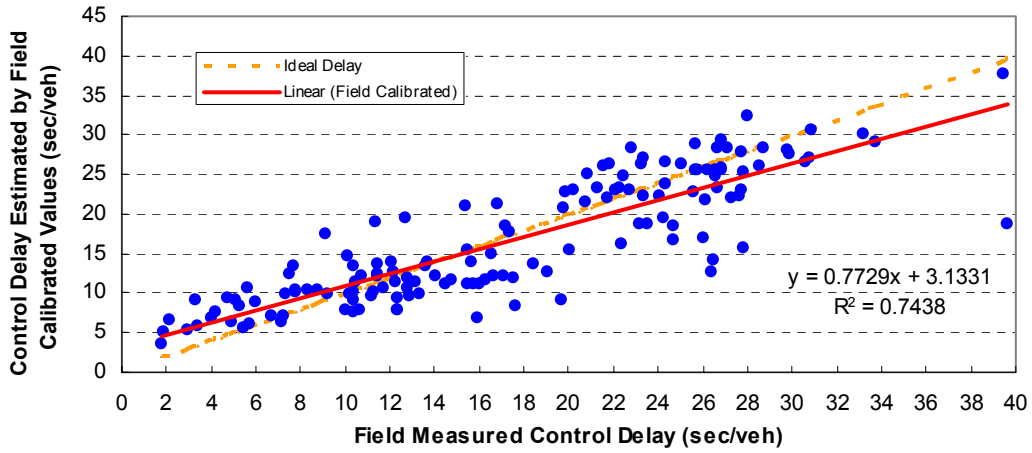

b) Comparison of control delay estimated using the HCM model with field calibrated values to the field measurements

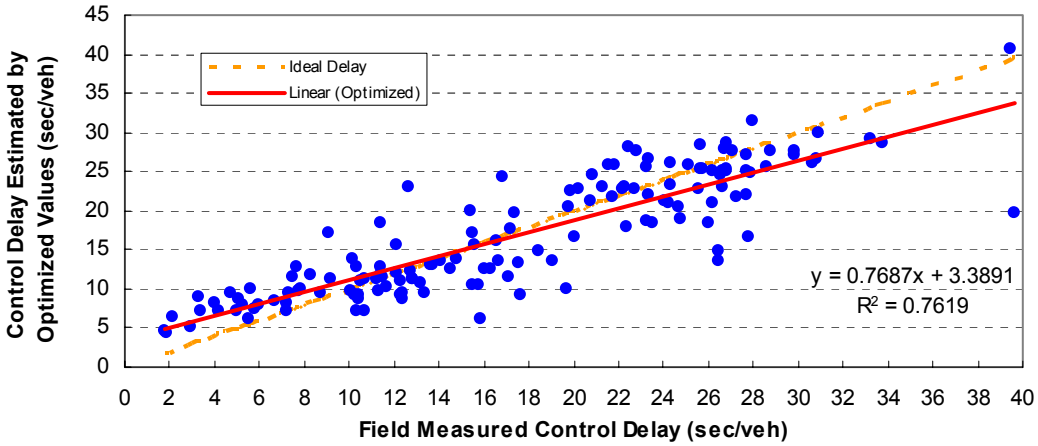

c) Comparison of control delay estimated using the HCM model with optimized values to the field measurements

Figure 4.20 Comparison of Control Delay Estimated Using the HCM Model to the Field Measurements for Through Lane Groups

Table 4.12 shows the statistics for the regression models corresponding to the plots shown in Figure 4.20. Ideally, the intercept should be equal to 0 and the slope should equal to 1. However, no matter which set of saturation flow rate and *kI*-value is used in the HCM control delay model, the intercept is greater than 0 and the slope is less than 1 at the 95% confidence interval (CI). This implies that the model overestimates the control delay when it is low, but underestimates it when it increases. Statistics for no-intercept regression models are also shown in Table 4.12. Table 4.12a indicates that when the HCM default values are used in the HCM delay model, the slope is greater than 1 and the control delay is overestimated. When field calibrated or optimized values are used, as shown in Table 4.12b and 4.12c, the slope is lower than 1 and the control delay is underestimated. The R^2 for the regression model with intercept is close to that for the model without intercept when field calibrated or optimized values are used.

Table 4.12 Statistical Relationship between Control Delay Estimated Using the HCM Model and the Field Measurements for Through Lane Groups

a). Statistical relationship between control delay estimated using the HCM model with the HCM default values and the field measurements

		With Intercept	Intercept = 0
R^2		0.5797	0.4245
Standard Error		5.3727	6.2650
Intercept	Coefficient	7.3671	0
	Standard Error	1.0173	N/A
	Lower 95% CI	5.3561	N/A
	Upper 95% CI	9.3781	N/A
Slope	Coefficient	0.7320	1.0721
	Standard Error	0.0523	0.0268
	Lower 95% CI	0.6286	1.0190
	Upper 95% CI	0.8353	1.1251

b). Statistical relationship between control delay estimated using the HCM model with field calibrated values and the field measurements

		With Intercept	Intercept = 0
R^2		0.7438	0.7115
Standard Error		3.9105362	4.1352
Intercept	Coefficient	3.1331	0
	Standard Error	0.7404	N/A
	Lower 95% CI	1.6694	N/A
	Upper 95% CI	4.5968	N/A
Slope	Coefficient	0.7729	0.9175
	Standard Error	0.0381	0.0177
	Lower 95% CI	0.6977	0.8825
	Upper 95% CI	0.8482	0.9526

c). Statistical relationship between control delay estimated using the HCM model with optimized values and the field measurements

		With Intercept	Intercept = 0
R^2		0.7619	0.7228
Standard Error		3.7045	3.9834
Intercept	Coefficient	3.3891	0
	Standard Error	0.7014	N/A
	Lower 95% CI	2.0025	N/A
	Upper 95% CI	4.7757	N/A
Slope	Coefficient	0.7687	0.9252
	Standard Error	0.0361	0.0171
	Lower 95% CI	0.6975	0.8915
	Upper 95% CI	0.8400	0.9589

- Permissive Left-turn Lane Group

Figures 4.21 shows the field measured control delays against estimated HCM control delay using the HCM default, field calibrated, and optimized saturation flow rates and *kI* values, respectively, for the permissive left-turn lane group. The solid line is the regression line and the dotted line represents the ideal relationship between them.

Figure 4.21a indicates that control delay estimated using the HCM default values is overestimated in most cases. However, when the field calibrated and optimized values are used, the model estimated control delay is lower than that from field measurements in most cases, as shown in Figures 4.21b and 4.21c.

No matter what values of the saturation flow rate and *kI* are used in the HCM control delay model, the estimated delays are scattered and the corresponding R^2 value is quite low. The HCM delay model may not accurately reflect the performance of the permissive left-turn movement.

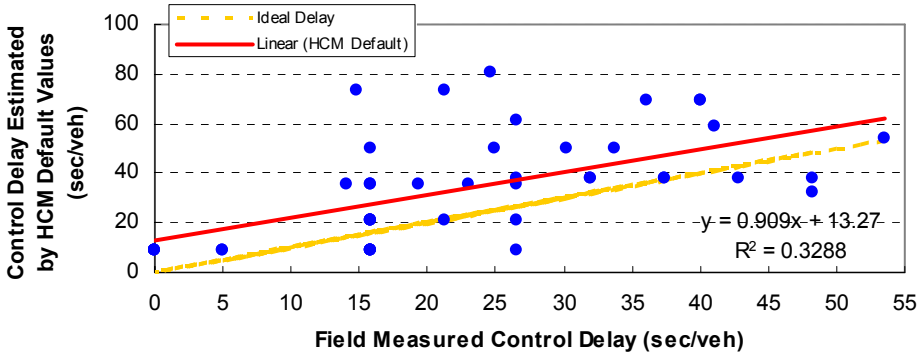

a) Comparison of control delay estimated using the HCM model with the HCM default values to the field measurements

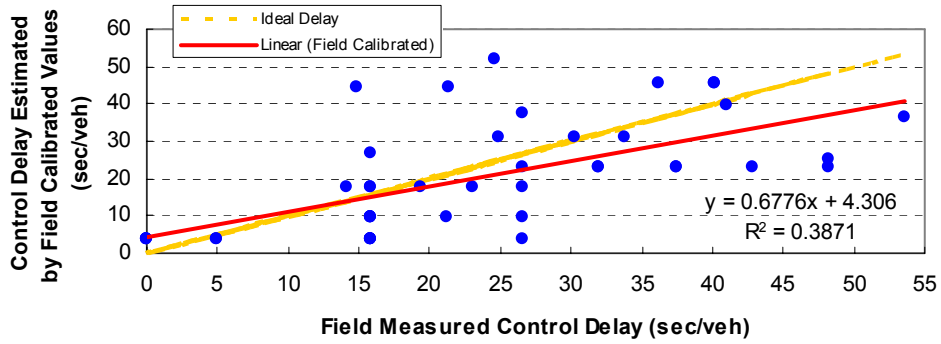

b) Comparison of control delay estimated using the HCM model with field calibrated values to the field measurements

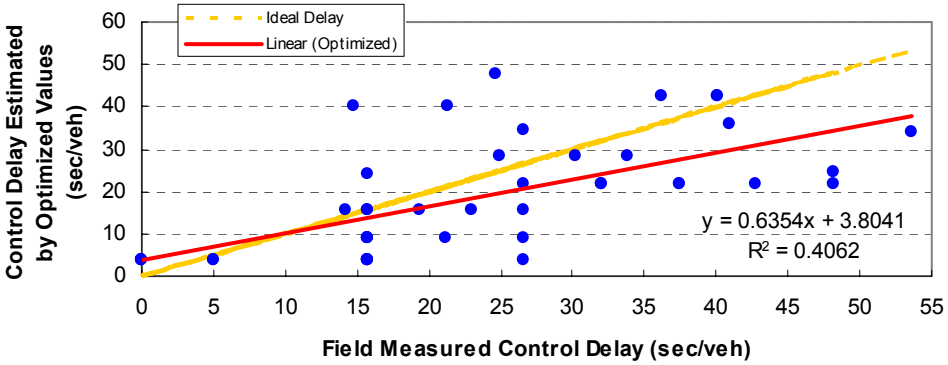

c) Comparison of control delay estimated using the HCM model with optimized values to the field measurements

Figure 4.21 Comparison of Control Delay Estimated Using the HCM Model to the Field Measurements for the Permissive Left-turn Lane Group

Table 4.13 shows the statistics for the regression models corresponding to the plots shown in Figure4.21. Ideally, as stated for the through lane groups, the intercept should be equal to 0 and the sloped should be equal to 1. When default values are used in the HCM model (Table 4.13a), the intercept is greater than 0 but the slope may be 1 at the 95% confidence interval, which implies that the model may overestimate the control delay. However, when field calibrated or optimized values are used in the model (Table 4.13b and 4.13c), the intercept may be 0 but the

slope is less than 1 at the 95% confidence interval. This indicates that the model may underestimate the control delay. Statistics for no-intercept regression models are also shown in Table 4.13. Table 4.13a indicates that when the HCM default values are used in the HCM delay model, the slope is greater than 1 and the control delay is overestimated. When field calibrated or optimized values are used, as shown in Table 4.13b and 4.13c, the slope is lower than 1 and the control delay is underestimated. What is obvious, however, is the very large uncertainty in the regression parameter estimates themselves.

Table 4.13 Statistical Relationship between Control Delay Estimated Using the HCM Model and the Field Measurements for Permissive Left-turn Lane Groups

a). Statistical relationship between control delay estimated using the HCM model with the HCM default values and the field measurements

		With Intercept	Intercept = 0
R^2		0.3288	0.2317
Standard Error		17.7638	18.7873
Intercept	Coefficient	13.2702	0
	Standard Error	5.3223	N/A
	Lower 95% CI	2.5367	N/A
	Upper 95% CI	24.0036	N/A
Slope	Coefficient	0.9090	1.3374
	Standard Error	0.1981	0.1042
	Lower 95% CI	0.5096	1.1274
	Upper 95% CI	1.3085	1.5475

b). Statistical relationship between control delay estimated using the HCM model with field calibrated values and the field measurements

		With Intercept	Intercept = 0
R^2		0.3871	0.3654
Standard Error		11.6616	11.7302
Intercept	Coefficient	4.3060	0
	Standard Error	3.4940	N/A
	Lower 95% CI	-2.7403	N/A
	Upper 95% CI	11.3524	N/A
Slope	Coefficient	0.6776	0.8166
	Standard Error	0.1300	0.0651
	Lower 95% CI	0.4153	0.6854
	Upper 95% CI	0.9398	0.9477

c). Statistical relationship between control delay estimated using the HCM model with optimized values and the field measurements

		With Intercept	Intercept = 0
R^2		0.4062	0.3860
Standard Error		10.5072	10.5620
Intercept	Coefficient	3.8041	0
	Standard Error	3.1481	N/A
	Lower 95% CI	-2.5447	N/A
	Upper 95% CI	10.1529	N/A
Slope	Coefficient	0.6354	0.7582
	Standard Error	0.1172	0.0586
	Lower 95% CI	0.3991	0.6401
	Upper 95% CI	0.8716	0.8763

In summary, when the field calibrated or the optimized saturation flow rate and *kI* are used, the control delay estimated by the HCM delay model accurately reflects the reality for through lane groups. However, the control delay estimated using the default saturation flow rate and *kI* may not be accurate enough. For the permissive left-turn lane group, even when the optimized saturation flow rate and *kI* are used, the R^2 is still very low and this indicates that the HCM delay model may not be trustable.

CHAPTER 5. CONCLUSIONS AND RECOMMENDATIONS

5.1 Conclusions

The following conclusions are drawn from the analysis of the control delay estimated using the HCM control delay model and the field measurement, in which the research questions listed in Chapter 1 are now addressed:

1) To what extent does the un-calibrated HCM saturation flow rate and corresponding delay model adequately predict field delay at signalized intersection?

The saturation flow rate calculated by the HCM equation with the default values appears to underestimate the calibrated field values for the study sites. As a consequence, the control delay estimated using the HCM model with the default values is higher than that obtained from the field measurements, and the control delay estimated based on the HCM default values may not accurately reflect the lane group performance.

From the analysis conducted it appears that the calibration of saturation flow rate is more critical than the calibration of *kI*-value. When properly calibrated saturation flow rate is used in the HCM control delay model, the average error in control delay between model estimate and field measurement decreases significantly. However, the contribution of calibrating *kI* to improving the model fit to the data is limited. In addition, the proportion of vehicles arriving on green or arrival type must be considered when vehicle arrivals are in platoons.

2) What is gained, in terms of prediction power, by using a field calibrated saturation flow rate and delay model parameters?

The field calibrated and optimized saturation flow rates appear to be very close. The field calibrated and optimized *kI* values are different, but their effects on control delay do not

appear to be significant. Control delays obtained from the HCM model using field calibrated and optimized saturation flow rates and *kI* values are close to those obtained from field measurements. Also, since the saturation flow rate is different from lane group to lane group, calibrating saturation flow rate for specific lane groups is necessary when the HCM control delay model is used. If a 5-second difference at an 80% assurance level is tolerable, the control delay estimated using the HCM model with calibrated saturation flow rate and *kI* value is reliable for evaluating the performance of through lane groups at signalized intersections.

Downstream queue affects the performance of through lane groups. When downstream queues are present, control delay for a through lane group increases significantly, even if the signal progression is good resulting in a large proportion of vehicles arriving on green. Therefore, under this circumstance, it is necessary that a deduction in the proportion of vehicles arriving on green be considered when the HCM control delay model is used.

3) What is the remaining error in predicting control delay when an optimal saturation flow rate and delay parameters are used?

Even when the optimized saturation flow rate and *kI*-value are used in the HCM control delay model, the R^2 is 0.762 for the through lane groups, which indicates that only 76.2% of the variability in field delays can be explained by the best calibrated model. The situation is even worse for the permissive left-turn lane group. Other factors in the delay model may also cause the inaccuracy. Further validation of the HCM control delay model form may be necessary, which is outside the scope of this thesis.

4) Are there differences in delay estimation for through and permitted left-turn lane groups?

In this research, the control delay for permissive left-turn lane groups estimated using the HCM model is not comparable with that obtained from field measurements due to the small sample size of the number of vehicles arriving per cycle. Therefore, additional sites and large sample size are needed to assess the reliability of the HCM control delay model for permissive left-turn lane groups.

5.2 Recommendations

The HCM control delay model gives general evaluations of the performance lane groups and/or signalized intersections. However, the characteristics of lane groups and/or intersections vary from site to site. Saturation flow rate, one of the most important variables in the HCM control delay model, affects the estimated control delay significantly, and it is also different from site to site. Therefore, calibrating saturation flow rate for specific studied lane groups and/or intersections is necessary in order to obtain accurate results when the HCM model is used to estimate control delay. In addition, the presence of downstream queue should be considered since it may affect the saturation flow rate of a studied intersection.

As described in the previous section, in this research, the control delay for left-turn lane group estimated using the HCM control delay model is not comparable with that obtained from field measurement due to the small size of samples for number of vehicles arriving per cycle. Further research, such as studying more sites with large size of sample data and using microscopic model in analysis, are needed for assessing the reliability of the HCM delay model for permissive left-turn lane group.

Only four lane groups are studied in this research, and they are in an urban area. The characteristics of isolated intersections in suburban or rural areas may be different. Additional signalized intersections and lane groups need to be selected to assess the reliability of the HCM control delay model across a variety of geographical settings.

CHAPTER 6. REFERENCE

1. Transportation Research Board. (2000) *Highway Capacity Manual*. National Research Council, Washington, D.C.

2. Koutsopoulos, H. N. and Toledo, T. (2004) *Statistical validation of traffic simulation models*. In 2004 Annual Meeting CD-ROM, Transportation Research Board, Washington, D. C.

3. Engelbrecht, R. J., Rambro, D. B., Rouphail, N. M., and Barkawi, A. A. (1997) *Validation of Generalized Delay Model for Oversaturated Conditions*. Transportation Research Record 1572, TRB, National Research Council, Washington, D, C., PP. 122-130.

4. Rouphail, N. M., Anwar, M., Fambro, D. B., Sloup, P., and Perez, C. E. (1997) *Validation of Generalized Delay Model for Vehicle-Actuated Traffic Signals*. Transportation Research Record 1572, TRB, National Research Council, Washington, D. C., PP. 105-111.

5. Bayarri, M. J., Berger, J. O., Higdon, D., Kennedy, M., Kottas, A., Paulo, R., Sacks, J., Cafeo, J. A., Cavendish, J. C., Lin, C-H., Tu, J. (2002) *A Framework for Validation of Computer Models*. Technical Report 128, NISS, www.niss.org/downloadabletechreports.html

6. Batista Paulo, R. M., Lin, J., Rouphail, N. M., and Sacks, J. (2004) *Calibrating and Validating Deterministic Traffic Models: Application to the HCM Control Delay at Signalized Intersections*. Proposed to present at the 84th Annual Meeting of the TRB, Washington, D. C.

7. Mousa, R. M., and Rouphail, N. M. (1989) *Effect of Platoons on Permissive Left-turn Capacity: Pilot Study*. Journal of Transportation Engineering. Volume 115, Issue 2, PP. 208-215.

8. Webster, F. V., and Cobbe, B. M. (1966) *Traffic Signals*. Her Majesty's Stationery Office, London, England.

APPENDIX A. SUMMARY OF FIELD MEASUREMENTS

Table A.1 Summary of Field Measurements for Southbound Through Lane Group at Wells-Grand Intersection

Cycle Number	Number of Vehicles	% Arrival on Green	Measured Delay (sec/veh)
1	22	30.4%	21.76
2	24	8.3%	28.02
3	22	26.1%	26.67
4	25	20.0%	26.82
5	21	19.0%	30.61
6	24	25.0%	20.85
7	21	23.8%	22.29
8	24	20.8%	21.83
9	18	11.1%	23.38
10	19	21.1%	22.15
11	21	27.3%	23.31
12	14	28.6%	23.21
13	22	17.4%	27.75
14	25	24.0%	23.28
15	23	21.7%	27.86
16	21	13.6%	27.10
17	16	0.0%	33.73
18	17	33.3%	23.52
19	17	21.1%	27.29
20	22	26.1%	21.27
21	16	11.8%	26.85
22	21	19.0%	24.34
23	15	20.0%	25.60
24	18	15.8%	25.78
25	21	30.4%	20.74
26	22	8.3%	30.87
27	21	13.0%	26.69
28	17	5.3%	29.84
29	21	22.7%	24.34
30	20	20.0%	26.18
31	20	18.2%	21.58
32	18	11.1%	30.80
33	18	15.8%	25.67
34	17	16.7%	26.54
35	18	27.8%	19.81
36	19	21.1%	22.72
37	18	22.2%	27.69
38	14	7.1%	28.56
39	25	17.9%	33.22
40	20	9.5%	25.66
41	21	13.6%	22.80
42	20	22.7%	20.26
43	16	12.5%	26.85
44	21	13.6%	28.74
45	20	13.6%	29.88
46	20	23.8%	19.86
47	13	7.1%	26.60
48	19	15.8%	25.09

Table A.2 Summary of Field Measurements for Southbound Through Lane Group at LaSalle-Ohio Intersection

Cycle Number	Number of Vehicles	% Arrival on green	Initial Queuing Vehicles	Measured Delay (sec/veh)
1	30	68.8%	0	5.63
2	37	78.9%	0	5.96
3	21	82.6%	0	2.97
4	21	65.2%	0	7.80
5	22	47.8%	0	9.11
6	11	63.6%	0	4.76
7	33	88.6%	0	1.92
8	33	61.8%	0	7.66
9	22	78.3%	0	2.12
10	27	75.0%	0	5.27
11	22	69.6%	0	3.33
12	27	46.9%	0	11.36
13	35	59.5%	0	10.14
14	35	73.0%	0	8.77
15	27	66.7%	0	11.70
16	35	66.7%	0	11.50
17	36	67.6%	0	7.48
18	36	63.9%	0	10.37
19	35	62.5%	0	11.42
20	36	53.8%	3	15.41
21	31	60.0%	0	13.61
22	33	79.4%	0	10.68
23	31	62.9%	0	12.15
24	27	64.3%	0	10.50
25	33	66.7%	0	12.82
26	30	71.0%	0	13.32
27	34	56.8%	2	17.21
28	32	64.7%	0	11.43
29	30	75.8%	2	7.76
30	28	70.0%	0	7.34
31	33	75.0%	0	10.38
32	33	75.0%	0	5.07
33	29	71.0%	0	10.21
34	26	76.7%	0	4.22
35	33	74.4%	0	12.35
36	36	70.3%	0	13.14
37	30	41.9%	6	24.09
38	33	47.1%	3	26.16
39	34	74.3%	2	10.71
40	34	66.7%	0	17.13
41	32	75.0%	2	15.53
42	28	71.9%	1	11.29
43	30	78.8%	0	10.34
44	32	71.4%	1	15.77
45	34	67.6%	2	13.68
46	33	82.9%	0	15.89
47	36	74.4%	0	10.42
48	31	66.7%	0	12.28

Table A.3 Summary of Field Measurements for Northbound Through Lane Group at LaSalle-Ontario Intersection

Cycle Number	Number of Vehicles	% Arrival on Green	Initial Queuing Vehicles	Measured Delay (sec/veh)
1	35	62.9%	0	12.11
2	30	80.0%	0	4.96
3	34	76.5%	0	12.32
4	29	55.2%	0	16.54
5	34	67.6%	0	16.63
6	36	72.2%	0	12.86
7	41	70.7%	0	14.75
8	32	90.6%	0	1.82
9	34	67.6%	0	14.06
10	34	88.2%	1	3.42
11	34	82.4%	0	5.77
12	28	82.1%	0	5.49
13	35	80.0%	0	6.70
14	32	78.1%	3	8.31
15	31	80.6%	0	7.19
16	31	71.0%	0	19.66
17	37	73.0%	6	12.68
18	37	78.4%	0	10.04
19	32	87.5%	2	4.00
20	33	78.8%	0	7.23
21	29	65.5%	0	16.28
22	35	71.4%	1	12.75
23	25	52.0%	5	27.81
24	38	50.0%	7	22.48
25	34	61.8%	3	22.35
26	29	58.6%	3	20.01
27	31	67.7%	5	15.47
28	33	69.7%	0	14.48
29	38	57.9%	0	24.74
30	30	56.7%	7	24.25
31	22	50.0%	3	26.45
32	33	51.5%	3	26.04
33	32	75.0%	3	16.01
34	25	44.0%	7	39.62
35	34	32.4%	17	39.46
36	33	63.6%	6	24.68
37	32	56.3%	9	27.71
38	27	66.7%	3	26.43
39	34	73.5%	1	9.22
40	37	73.0%	0	11.19
41	37	64.9%	6	16.85
42	31	64.5%	2	18.40
43	30	73.3%	4	17.54
44	27	66.7%	3	19.05
45	34	64.7%	5	17.35
46	35	77.1%	0	12.37
47	31	71.0%	5	15.63
48	29	72.4%	0	17.60

Table A.4 Summary of Field Measurements for Northbound Left-turn Lane Group at LaSalle-Grand Intersection

Cycle Number	Number of Vehicles	% Arrival on Green	Measured Delay (sec/veh)
1	2	100.0%	15.80
2	1	100.0%	26.60
3	2	50.0%	32.00
4	1	100.0%	15.80
5	1	100.0%	0.00
6	3	100.0%	19.40
7	4	100.0%	15.80
8	2	50.0%	48.20
9	4	50.0%	36.15
10	1	0.0%	48.20
11	2	100.0%	15.80
12	3	66.7%	30.20
13	1	100.0%	15.80
14	3	100.0%	23.00
15	3	66.7%	33.80
16	3	66.7%	24.93
17	2	100.0%	15.80
18	1	100.0%	5.00
19	2	50.0%	26.60
21	3	100.0%	26.60
22	2	50.0%	42.80
23	3	33.3%	41.00
24	4	50.0%	40.10
25	4	50.0%	40.10
27	2	100.0%	26.60
28	2	100.0%	15.80
29	1	100.0%	0.00
30	2	50.0%	37.40
32	2	50.0%	32.00
33	2	100.0%	21.20
34	5	60.0%	24.60
35	1	100.0%	0.00
36	5	80.0%	14.80
37	4	75.0%	26.60
38	2	0.0%	53.60
39	3	100.0%	14.13
40	1	100.0%	0.00
41	1	100.0%	15.80
42	3	100.0%	15.80
43	1	100.0%	5.00
44	1	100.0%	15.80
45	1	100.0%	15.80
46	3	100.0%	15.80
47	5	80.0%	21.28
48	2	50.0%	37.40

APPENDIX B. FIELD MEASUREMENT OF INTERSECTION CONTROL DELAY

The method is according to Chapter 16, HCM2000 (1). The information is collected including:

- Vehicle-in-queue

  The survey should begin at the start of the red phase of the lane group. The count includes vehicles arriving when the signal is actually green but stopped because vehicles in front have not yet started moving. A vehicle is considered as having joined the queue when it approaches within one car length of a stopped vehicle and is itself about to stop. All vehicles that join a queue are then included in the vehicle-in-queue counts until they cross the stop line.

- Count Interval

  At regular intervals of between 10 and 20 seconds, records the number of vehicles in queue. The regular intervals should not be an integral divisor of the cycle length.

- Number of Vehicles Arriving and Stopping

  During the entire survey period, maintains separate volume counts of total vehicles arriving during the survey period and total vehicles arriving during the survey period that stop one or more times.

Input all information onto the spreadsheet. Table A.5 is an example of worksheet for computation of control delay.

APPENDIX C. SUMMARY OF LANE GROUP CONTROL DELAY

Table C.1 Summary of Control Delay (sec/veh) for Southbound Through Lane Group at Wells-Grand Intersection

Cycle Number	Number of Vehicles	Parameters in the HCM model			Field Measurement
		Default	Field Calibrated	Optimized	
1	22	25.01	22.03	21.73	21.76
2	24	36.38	32.34	31.46	28.02
3	22	26.35	23.32	22.96	26.67
4	25	33.65	29.37	28.54	26.82
5	21	29.34	26.50	26.05	30.61
6	24	28.82	25.07	24.54	20.85
7	21	26.09	23.35	23.03	22.29
8	24	30.16	26.36	25.76	21.83
9	18	29.08	27.00	26.61	23.38
10	19	25.18	22.98	22.71	22.15
11	21	25.05	22.35	22.06	23.31
12	14	19.86	18.68	18.58	23.21
13	22	30.91	27.73	27.19	27.75
14	25	30.36	26.21	25.54	23.28
15	23	28.73	25.31	24.82	27.86
16	21	31.08	28.19	27.67	27.10
17	16	30.73	29.01	28.61	33.73
18	17	20.31	18.65	18.53	23.52
19	17	23.69	21.95	21.73	27.29
20	22	26.35	23.32	22.96	21.27
21	16	27.32	25.68	25.37	26.85
22	21	29.34	26.50	26.05	24.34
23	15	24.27	22.86	22.64	25.60
24	18	27.67	25.62	25.28	25.78
25	21	24.10	21.43	21.18	20.74
26	22	33.90	30.61	29.95	30.87
27	21	31.27	28.37	27.85	26.69
28	17	30.00	28.10	27.71	29.84
29	21	26.41	23.67	23.33	24.34
30	20	28.08	25.56	25.17	26.18
31	20	28.66	26.11	25.71	21.58
32	18	29.08	27.00	26.61	30.80
33	18	27.67	25.62	25.28	25.67
34	17	26.62	24.81	24.51	26.54
35	18	22.52	20.61	20.43	19.81
36	19	25.18	22.98	22.71	22.72
37	18	24.08	22.13	21.90	27.69
38	14	27.23	25.92	25.64	28.56
39	25	34.41	30.09	29.23	33.22
40	20	31.38	28.76	28.25	25.66
41	21	31.08	28.19	27.67	22.80
42	20	25.52	23.07	22.78	20.26
43	16	27.10	25.47	25.17	26.85
44	21	31.08	28.19	27.67	28.74
45	20	30.09	27.50	27.04	29.88
46	20	25.20	22.76	22.48	19.86
47	13	26.58	25.42	25.17	26.60
48	19	28.51	26.21	25.83	25.09

Table C.2 Summary of Control Delay (sec/veh) for Southbound Through Lane Group at LaSalle-Ohio Intersection

Cycle Number	Number of Vehicles	Parameters in the HCM model			Field Measurement
		Default	Field Calibrated	Optimized	
1	30	14.28	10.59	10.10	5.63
2	37	15.17	8.79	8.01	5.96
3	21	6.63	5.37	5.15	2.97
4	21	11.85	10.23	9.97	7.80
5	22	19.82	17.47	17.15	9.11
6	11	10.07	9.48	9.38	4.76
7	33	9.01	4.94	4.40	1.92
8	33	18.65	13.38	12.74	7.66
9	22	8.17	6.69	6.44	2.12
10	27	10.79	8.23	7.86	5.27
11	22	10.82	9.14	8.87	3.33
12	27	22.60	18.91	18.44	11.36
13	35	21.08	14.62	13.87	10.14
14	35	16.05	10.27	9.58	8.77
15	27	13.51	10.70	10.30	11.70
16	35	18.40	12.30	11.58	11.50
17	36	18.78	12.27	11.49	7.48
18	36	20.16	13.46	12.67	10.37
19	35	19.95	13.64	12.90	11.42
20	36	36.26	21.07	19.98	15.41
21	31	17.90	13.47	12.92	13.61
22	33	12.30	7.82	7.25	10.68
23	31	16.90	12.59	12.04	12.15
24	27	14.29	11.40	11.00	10.50
25	33	16.88	11.83	11.21	12.82
26	30	13.52	9.91	9.43	13.32
27	34	31.38	18.57	17.72	17.21
28	32	16.90	12.23	11.65	11.43
29	30	18.12	10.38	9.76	7.76
30	28	12.86	9.87	9.45	7.34
31	33	13.89	9.21	8.62	10.38
32	33	13.89	9.21	8.62	5.07
33	29	13.01	9.74	9.29	10.21
34	26	9.87	7.60	7.26	4.22
35	33	14.12	9.41	8.82	12.35
36	36	17.77	11.39	10.62	13.14
37	30	33.76	22.18	21.33	24.09
38	33	31.91	21.80	20.98	26.16
39	34	31.38	12.01	11.13	10.71
40	34	17.61	12.06	11.39	17.13
41	32	28.25	11.15	10.41	15.53
42	28	14.24	10.09	9.62	11.29
43	30	10.84	7.52	7.07	10.34
44	32	26.14	11.08	10.44	15.77
45	34	31.38	13.84	12.97	13.68
46	33	11.06	6.74	6.17	15.89
47	36	16.23	10.06	9.31	10.42
48	31	15.58	11.42	10.88	12.28

Table C.3 Summary of Control Delay (sec/veh) for Northbound Through Lane Group at LaSalle-Ontario Intersection

Cycle Number	Number of Vehicles	Parameters in the HCM model			Field Measurement
		Default	Field Calibrated	Optimized	
1	35	15.93	14.02	15.56	12.11
2	30	7.40	6.28	7.23	4.96
3	34	9.53	7.94	9.27	12.32
4	29	16.26	15.01	16.01	16.54
5	34	13.79	12.07	13.47	16.63
6	36	11.58	9.67	11.25	12.86
7	41	14.47	11.63	13.92	14.75
8	32	4.68	3.45	4.51	1.82
9	34	13.79	12.07	13.47	14.06
10	34	7.53	5.72	7.17	3.42
11	34	7.70	6.17	7.46	5.77
12	28	6.38	5.44	6.24	5.49
13	35	8.75	7.05	8.47	6.70
14	32	12.31	10.32	11.81	8.31
15	31	7.44	6.23	7.26	7.19
16	31	10.31	9.02	10.10	19.66
17	37	24.93	19.49	23.03	12.68
18	37	9.97	7.96	9.63	10.04
19	32	8.52	6.76	8.12	4.00
20	33	8.52	7.07	8.29	7.23
21	29	12.84	11.67	12.63	16.28
22	35	12.71	10.69	12.29	12.75
23	25	16.92	15.70	16.62	27.81
24	38	29.58	24.77	28.21	22.48
25	34	18.44	16.22	17.91	22.35
26	29	16.84	15.40	16.52	20.01
27	31	17.63	15.51	17.07	15.47
28	33	12.69	11.13	12.41	14.48
29	38	19.30	16.81	18.79	24.74
30	30	21.63	19.48	21.03	24.25
31	22	15.06	14.23	14.88	26.45
32	33	18.89	16.90	18.43	26.04
33	32	13.02	11.05	12.54	16.01
34	25	20.07	18.68	19.70	39.62
35	34	42.15	37.66	40.73	39.46
36	33	21.28	18.52	20.48	24.68
37	32	26.04	22.93	25.08	27.71
38	27	13.95	12.71	13.67	26.43
39	34	11.66	9.82	11.29	9.22
40	37	11.74	9.67	11.38	11.19
41	37	25.74	21.16	24.24	16.85
42	31	15.23	13.65	14.89	18.40
43	30	13.68	11.86	13.21	17.54
44	27	13.95	12.71	13.67	19.05
45	34	20.42	17.63	19.63	17.35
46	35	9.65	7.93	9.36	12.37
47	31	16.14	13.92	15.53	15.63
48	29	9.37	8.28	9.19	17.60

Table C.4 Summary of Control Delay (sec/veh) for Northbound Permissive Left-turn Lane Group at LaSalle-Grand Intersection

Cycle Number	Number of Vehicles	Parameters in the HCM model			Field Measurement
		Default	Field Calibrated	Optimized	
1	2	21.21	9.55	8.96	15.80
2	1	9.07	3.77	3.69	26.60
3	2	37.74	22.89	21.57	32.00
4	1	9.07	3.77	3.69	15.80
5	1	9.07	3.77	3.69	0.00
6	3	35.23	17.43	15.81	19.40
7	4	50.23	26.84	23.90	15.80
8	2	37.74	22.89	21.57	48.20
9	4	68.98	45.59	42.65	36.15
10	1	32.08	25.01	24.46	48.20
11	2	21.21	9.55	8.96	15.80
12	3	49.60	31.15	28.11	30.20
13	1	9.07	3.77	3.69	15.80
14	3	35.23	17.43	15.81	23.00
15	3	49.60	31.15	28.11	33.80
16	3	49.60	31.15	28.11	24.93
17	2	21.21	9.55	8.96	15.80
18	1	9.07	3.77	3.69	5.00
19	2	37.74	22.89	21.57	26.60
21	3	35.23	17.43	15.81	26.60
22	2	37.74	22.89	21.57	42.80
23	3	58.48	39.62	35.71	41.00
24	4	68.98	45.59	42.65	40.10
25	4	68.98	45.59	42.65	40.10
27	2	21.21	9.55	8.96	26.60
28	2	21.21	9.55	8.96	15.80
29	1	9.07	3.77	3.69	0.00
30	2	37.74	22.89	21.57	37.40
32	2	37.74	22.89	21.57	32.00
33	2	21.21	9.55	8.96	21.20
34	5	80.76	52.20	47.83	24.60
35	1	9.07	3.77	3.69	0.00
36	5	73.26	44.70	40.33	14.80
37	4	61.01	37.63	34.68	26.60
38	2	54.26	36.22	34.17	53.60
39	3	35.23	17.43	15.81	14.13
40	1	9.07	3.77	3.69	0.00
41	1	9.07	3.77	3.69	15.80
42	3	35.23	17.43	15.81	15.80
43	1	9.07	3.77	3.69	5.00
44	1	9.07	3.77	3.69	15.80
45	1	9.07	3.77	3.69	15.80
46	3	35.23	17.43	15.81	15.80
47	5	73.26	44.70	40.33	21.28
48	2	37.74	22.89	21.57	37.40

APPENDIX D. CONTROL DELAY ESTIMATED BY THE HCM MODEL USING THE CYCLE-BY-CYCLE SATURATION FLOW RATE FOR NORTHBOUND LEFT-TURN LANE GROUP AT LASALLE-GRAND INTERSECTION

Table D.1 The Control Delay Estimated by the HCM Model Using the Cycle-by-cycle Saturation Flow Rate

Cycle Number	Number of LT Vehicles	Number of Opposing Vehicles	Saturation Flow Rate (veh/h)	Control Delay (sec/veh)	
				Estimated by the HCM Model	Field Measurement
1	2	39	169	29.86	15.80
2	1	32	169	13.23	26.60
3	2	34	174	47.19	32.00
4	1	32	169	13.23	15.80
5	1	32	216	8.26	0.00
6	3	42	169	48.11	19.40
7	4	33	169	67.12	15.80
8	2	38	169	48.61	48.20
9	4	31	191	75.00	36.15
10	1	33	169	37.88	48.20
11	2	36	169	29.86	15.80
12	3	32	223	45.23	30.20
13	1	33	169	13.23	15.80
14	3	30	185	41.86	23.00
15	3	27	218	46.44	33.80
16	3	28	287	33.15	24.93
17	2	32	169	29.86	15.80
18	1	32	191	10.50	5.00
19	2	35	213	36.03	26.60
21	3	26	219	31.82	26.60
22	2	34	169	48.61	42.80
23	3	34	219	55.07	41.00
24	4	32	195	73.30	40.10
25	4	26	287	47.90	40.10
27	2	35	169	29.86	26.60
28	2	27	244	15.47	15.80
29	1	32	226	7.55	0.00
30	2	27	235	31.55	37.40
32	2	26	222	34.05	32.00
33	2	30	208	20.84	21.20
34	5	21	417	34.94	24.60
35	1	21	444	1.85	0.00
36	5	20	428	26.41	14.80
37	4	23	320	34.68	26.60
38	2	26	203	55.26	53.60
39	3	21	361	12.34	14.13
40	1	28	263	5.55	0.00
41	1	25	322	3.65	15.80
42	3	27	241	26.97	15.80
43	1	28	261	5.64	5.00
44	1	27	290	4.54	15.80
45	1	27	193	10.29	15.80
46	3	26	226	30.16	15.80
47	5	20	361	33.90	21.28
48	2	26	274	25.91	37.40